The geomorphic imprint of glacier surges into open-marine waters: Examples from eastern Svalbard

D. Ottesen[1], J.A. Dowdeswell[2], V.K. Bellec[1] and L.R. Bjarnadóttir[1]

[1] Geological Survey of Norway, Postboks 6315 Torgard, N-7491 Trondheim, Norway

[2] Scott Polar Research Institute, University of Cambridge, Cambridge CB2 1ER, UK

Abstract

Seafloor morphology beyond nine tidewater glaciers terminating in open-marine settings in eastern Svalbard has been investigated using multibeam swath-bathymetry. Historical information on tidewater glacier fluctuations over the past century or so shows that the seafloor offshore has been exposed only recently. Most glaciers have been observed to surge or have looped surface moraines indicating past surges. During these ice advances and subsequent retreat, a well-preserved submarine landform assemblage has been produced. (a) Subglacial landforms include: overridden moraine ridges, mega-scale glacial lineations (MSGLs), other streamlined lineations, elongate drumlins and medial moraines, small ridges forming a complex boxwork or rhombohedral pattern, and meltwater-related eskers and channels. (b) Ice-marginal landforms include: large terminal moraines with debris flow lobes on their outer flanks and indentations on their inner sides, small transverse retreat moraines, and crater-like kettle holes. (c) Glacimarine features include: iceberg ploughmarks and an otherwise relatively smooth sedimentary seafloor produced by fine-grained debris rain-out. A schematic plan-view landform assemblage model for tidewater glaciers advancing into open-marine settings is developed. Arcuate terminal moraines marking the ice-advance limit provide a distinctive component. Submarine basin(s) exposed inside these moraine ridges when ice retreats contain suites of individual landforms, produced subglacially and ice-marginally, with a consistent order of timing of deposition and stratigraphic superposition. The new schematic model is compared with earlier models based on submarine landforms associated with surges in the more topographically constrained setting of Spitsbergen fjords. Differences include: (i) the overall arcuate shape of the open-marine assemblage; (ii) the indented ice-proximal sides of terminal moraine ridges; (iii) the fan-shaped pattern of streamlined lineations; (iv) crater-like kettle holes at the inner lateral margins of many submarine basins; (v) prominent systems of eskers and channels. Modern glaciological analogues from ongoing surges of ice caps in eastern Svalbard and Severnaya Zemlya provide contemporary observations of ice advance into open-marine settings, including heavily crevassed ice lobes with finger-like termini.

1. Introduction

Many Svalbard glaciers are of surge-type, undergoing brief rapid advance in an active phase followed by decades of stagnation and retreat during a quiescent phase (e.g. Liestøl, 1969; Schytt, 1969; Dowdeswell et al., 1991, 1995; Hagen et al., 1993; Hamilton and Dowdeswell, 1996; Jiskoot et al., 2000; Sund et al., 2014). The geological imprint of recent glacier surges on the seafloor of several steep-sided fjords in Svalbard has been investigated using high-resolution multibeam swath-bathymetric data (e.g. Ottesen and Dowdeswell, 2006; Ottesen et al., 2008; Flink et al., 2015, 2017; Streuff et al., 2015; Dowdeswell and Ottesen, 2016a; Fransner et al., 2017). By contrast, and despite the examination of early side-scan sonar data from offshore of the surging Austfonna ice cap (e.g. Solheim, 1985, 1991; Solheim and Pfirman, 1985; Dowdeswell et al., 2008), the submarine landform record from glaciers surging into the topographically less constrained open-marine environment of eastern Svalbard is less well-known (Robinson and Dowdeswell, 2011; Dowdeswell et al., 2016a). It is important that the assemblages of landforms characteristic of surging glaciers in both marine and terrestrial environments are described and understood (e.g. Sharp, 1985a, 1985b; Evans and Rea, 2003; Ottesen and Dowdeswell, 2006; Ottesen et al., 2008; Sund et al., 2009), so that glacier advances due to surging, driven by internal glaciological processes (e.g. Kamb et al., 1985; Kamb, 1987; Raymond, 1987; Fowler et al., 2001; Murray et al., 2003; Sevestre and Benn, 2015), can be distinguished from those of climatically driven glacier fluctuations in the geological record.

In this paper, we describe and discuss the detailed seafloor morphology in front of nine glaciers that terminate in relatively open-marine settings in eastern Svalbard; most of these tidewater glaciers have either been observed to surge or have looped surface moraines and ice structures indicative of surge-type glaciers (Meier and Post, 1969; Hagen et al., 1993). Eight of the glaciers drain from the large, complex ice cap covering most of Olav V Land in eastern Spitsbergen; the largest is Negribreen which is fed from a basin of about 1,100 km^2 and has retreated about 20 km since a surge advance in the 1930s (Liestøl, 1969). In total, the coastline around Olav V Land in our study area is 140 km long, with 35 km or 25% made up of marine-terminating glaciers. The ninth glacier is Besselsbreen, a 140 km^2 tidewater glacier draining the northern side of a 600 km^2 ice cap on Barentsøya (Fig. 1) (Hagen et al., 1993; Dowdeswell and Bamber, 1995). Evidence from 1936 oblique aerial photographs and early maps demonstrates that the seafloor between about 5-20 km beyond the present glacier termini has been exposed for less than a century or so in most cases. The submarine geomorphology is very well preserved, providing a suite of glacial landforms relating to the last major advance or surge of each glacier drainage basin. The assemblage and relative chronology of the landforms is presented here, together with a simple model of the geomorphic imprint produced by these glaciers.

2. Data Sources and Methods

Detailed multibeam swath-bathymetric data were collected by the Norwegian Hydrographic Service (NHS) east of Spitsbergen during the years 2007, 2008 and 2009. The data cover the seafloor around Olav V Land, at the head of Storfjorden, and offshore of northern Barentsøya (Fig. 1). The data were acquired to international hydrographic standards using Kongsberg EM3000, EM3002 or EM710 multibeam echo-sounders and were initially processed by the NHS for tidal corrections and the removal of false data points and artefacts. These regional data were gridded with a cell-size of 10 m, but we also have access to the raw data, which enabled us to reprocess and grid the data with 1 m or 2 m cell-size. Our mapping of seafloor glacial landforms uses a 2 m grid-cell size, and has a vertical resolution of better than 1 m. A more detailed technical review of multibeam echo-sounding is given in Jakobsson et al. (2016).

Historical information on the fluctuations of the tidewater glaciers of Olav V Land over the past century or so, in the form of early maps and aerial photographs, has been compiled by Lefauconnier and Hagen (1991). It should be noted that no aerial photographs were acquired before 1936, when the archipelago was comprehensively covered by oblique photographs (held in the collection of Norsk Polarinstitutt). The oblique geometry of the 1936 aerial photographs makes accurate mapping difficult, with vertical photography only beginning after WWII in Svalbard. Older ice-front positions were sketched by early explorers relative to observed features on adjacent land.

3. Results: the variety of submarine landforms offshore of Olav V Land

We describe the submarine landforms in front of eight glaciers or glacier systems in Olav V Land, eastern Spitsbergen, and Besselsbreen on Barentsøya (Fig. 1). These glaciers have all surged or advanced in the recent past, either in the 19th or 20th century. During these surges, a suite of landforms has been produced on the seafloor. The individual landform types may be divided into those formed subglacially, ice marginally and beyond the ice front in a glacier-influenced marine setting (e.g. Benn and Evans, 2010; Dowdeswell et al., 2016b). Most are sedimentary features at or close to the seafloor, sometimes buried by a thin cover of overlying fine-grained material derived mainly from suspension-settling from turbid glacial or glacifluvial meltwater plumes (e.g. Powell, 1990; Mugford and Dowdeswell, 2011); little bedrock is exposed at the seafloor offshore of Olav V Land, except as a few small islands and isolated submarine ridges. The submarine landforms and their mechanisms of formation are discussed generally before the distribution of landforms associated with each individual glacier is described in detail. Finally, the landform assemblages and their glaciological significance, as well as their links to the recent glacial history of the area, are discussed.

3.1 Subglacial Landforms

Several types of streamlined sedimentary landforms are found beyond the modern margins of the nine glaciers. Both curvilinear mega-scale glacial lineations (MSGLs) and blunt-nosed elongate drumlins are observed (Fig. 2A-B), and are interpreted to form by deformation of a soft till bed beneath ice that is either fast-flowing or transitional between relatively slow- and fast-moving ice (e.g. Clark, 1993, 1994; Wellner et al., 2001; Ó Cofaigh et al., 2002, 2005; Dowdeswell et al., 2004, 2016b; Clark et al., 2009; King et al., 2009; Spagnolo et al., 2014). Some of the elongate landforms appear to be transitional between classical MSGLs and drumlinoid features (Fig. 2A, B), forming part of a continuum of subglacial streamlining (e.g.

Clark, 1993; Dunlop and Clark, 2006). Medial moraine ridges are a further, and sometimes streamlined, submarine landform probably produced from a combination of supraglacial and subglacial sediment sources (Fig. 2C). Such features first form where glaciers from adjacent valleys flow together, and sediment is incorporated and transported at the interface between the two ice-flow units (e.g. Benn and Evans, 2010; Dowdeswell, E.K. et al., 2016).

Some smaller ridges just a few metres high, observed in eastern Svalbard waters, form a complex boxwork or rhombohedral pattern, with ridges orientated both transverse and sub-parallel to flow (Fig. 2D). They are interpreted as a result of the squeezing of soft sediments into subglacial crevasses near the ice margin (e.g. Solheim and Pfirman, 1985; Solheim, 1991; Dowdeswell et al., 2016a). These delicate landforms are preserved as largely stagnant ice thins and floats off as icebergs, typically in the early quiescent phase of a glacier surge.

In addition, two specifically meltwater-related subglacial landforms are observed. The first are often-sinuous ridges, interpreted as eskers (Fig. 2E), which represent the depositional sedimentary fill of channels cut upwards into overlying ice, known as R-channels (e.g. Röthlisberger, 1972; Benn and Evans, 2010; Dowdeswell and Ottesen, 2016b; Greenwood et al., 2016). The second are channels eroded into the sedimentary seafloor (e.g. Lowe and Anderson, 2003) (Fig. 2F), known as N-channels (Nye, 1976). The eskers and channels both have long-profiles that, unlike open river channels, trend both up- and down-slope, indicating that they were formed under high water pressure in confining subglacial meltwater systems (Shreve, 1972).

3.2 Ice-Marginal Landforms

These landforms, produced at or close to grounded tidewater glacier termini, include a variety of moraine ridges, ranging in size from large ridges tens of metres in height (Fig. 3A) to delicate landforms only a few metres in elevation and often spaced just a few tens of metres apart (Fig. 3B). The large ridges sometimes occur as individual landforms but are also found as small numbers of sub-parallel landforms. The small ridges usually occur in clusters of tens and even hundreds of individual landforms. The large ridges and many of the smaller ridges are orientated transverse to the direction of past ice flow (Fig. 3A-B). They contrast with the more complex clusters of small crevasse-fill ridges with multiple orientations in a boxwork structure (Fig. 2D).

The large transverse ridges are interpreted as terminal or end moraines, formed at the maximum position of grounded ice advance, for example at the end of a glacier surge or linked to Little Ice Age or full-glacial advances (e.g. Benn and Evans, 2010; Dowdeswell et al., 2016c; Graham and Hodgson, 2016). They may also be deposited at tidewater glacier termini when still-stands of decades or more during deglaciation allow sedimentary ridges to build at temporarily stable ice margins (e.g. Lønne et al., 2001). Subsequent ice readvances may deposit streamlined subglacial landforms on the surface of such large ridges, and renewed deglaciation may also contribute to the development of small transverse ridges on their crests (Fig. 3C).

The often steeper ice-distal flanks of these large ridges are typically associated with well-defined lobate landforms (Fig. 3E) (e.g. Ottesen and Dowdeswell, 2006; Dowdeswell et al., 2016d). These lobate landforms sometimes have blocky elements and flow structures visible at their surfaces and can be seen to override one another. They are interpreted as glacigenic debris-flow lobes linked to the rapid delivery and failure of soft subglacial sediments at former ice margins. They are often up to a few kilometres in length and up to a few tens of metres in thickness.

The smaller transverse ridges (Fig. 3B), usually found in sub-parallel clusters, are interpreted to have been formed in association with small winter readvances of tidewater glacier termini superimposed on longer-term summer retreat linked to iceberg calving (Boulton, 1986; Boulton et al., 1996; Ottesen and Dowdeswell, 2006; Todd et al., 2007; Flink et al., 2015; Dowdeswell and Ottesen, 2016b; Todd, 2016). This processes requires active, but not necessarily fast-flowing ice to generate the small winter readvances of the terminus, which push up the small ridges when iceberg calving is largely suppressed by the presence of winter sea ice. The ridges may be, but are not always, deposited annually (e.g. Ottesen and Dowdeswell, 2006; Burton et al., 2016).

Further ice-marginal landforms are the distinctive flat-floored crater-like depressions with relatively steep sides, known as kettle holes (Fig. 3F) (e.g. Eilertsen et al., 2016). They form when stagnant blocks of inactive glacier ice remain stranded in very shallow water after ice retreat, especially if the ice is rich in debris. After the ice blocks melt or float off in the marine environment, these depressions are often partly filled by fine-grained sediments from turbid glacial meltwater, further smoothing the crater-like floor.

3.3 Glacimarine Landforms

In the marine waters beyond tidewater glacier margins, the submarine keels of drifting icebergs may impinge on the sedimentary seafloor, forming irregular to chaotic patterns of depressions known as ploughmarks, sometimes with berms at either side (Fig. 4A) (e.g. Woodworth-Lynas et al., 1991; Dowdeswell et al., 1993; Bjarnadóttir et al., 2016). Where icebergs have multiple keels, parallel sets of ploughmarks are formed (e.g. Andreassen et al., 2014; Batchelor et al., 2016). Individual ploughmarks in our study area are metres to tens of metres wide and up to several hundred metres in length. Where icebergs wallow at a single point for hours to days, distinctive grounding pits are produced in the sedimentary seafloor (e.g. Barrie et al., 1992).

Glacimarine sedimentation by the rain-out of fine-grained debris from meltwater plumes begins to bury seafloor glacial landforms subsequent to their formation (Fig. 4B), and, in the case of subglacial landforms, after exposure by glacier retreat (e.g. Dowdeswell and Vásquez, 2013). The elapsed time since formation and the rate of glacimarine sediment delivery control the depth of burial. In the case of inner Storfjorden, most of the landforms inside the larger terminal moraines have been exposed for less than about a century, so burial depth beneath draping glacimarine sediment is inferred to be very limited based on the clear visibility of fine-scale features on the modern seafloor. An exception is the area close to the narrow passage between Spitsbergen, Barentsøya and several smaller islands (Fig. 1), Heleysundet, where tidally related current speeds reach more than 5 kts. Here, draping sediment cover appears thicker and an active sedimentary body of ripple-topped drift (Fig. 4C) can been seen to have built up to completely cover any glacial landforms (Fig. 4D).

4. Results: landforms and glacier fluctuations offshore of surge-type glaciers

4.1 Negribreen - submarine landforms

Multibeam swath-bathymetric imagery of the submarine glacial landforms in the open-marine setting offshore of the present terminus of Negribreen is shown in Figure 5A, and the distribution of these landforms is mapped in Figure 5B. A variety of subglacial and ice marginal landforms is present, as described below.

Large transverse moraine ridges and debris-flow lobes. Several large moraine ridges are observed offshore of the modern terminus of Negribreen (Fig. 5A-B). Unfortunately, however, the central part of the outmost moraine ridge is beyond the coverage of existing multibeam bathymetry. The terminal moraine ridge that defines the whole Negribreen submarine basin is estimated to be about 32 km long. The western part of the outer ridge is composed of two parts (Fig. 5A-B). The outermost part (labelled (1) in Figure 5A), is located close to the 1936 ice-front position mapped by Lefauconnier and Hagen (1991). This ridge has an arcuate form and transitions into a large set of debris-flow lobes. It is about 1 km wide and up to 15 m high. The second ridge (labelled (2) in Figure 5A), lies 2 to 4 km inshore of the first, is up to 1.5 km wide and 25 m high with a crest at between 50 and 65 m water depth. The eastern ridge complex is composed of up to six individual ridge crests, which may be linked to glacitectonic thrusting. The whole ridge complex is up to 2.5 km wide and 25 m high with individual crests about 200 m wide and 10 m high. The outermost terminal ridges have debris-flow lobes extending up to 2.5 km downslope onto the relatively smooth and sometimes iceberg-ploughed deeper-basin sediments further offshore beyond the extent of recent glacier fluctuations. Downslope-orientated flow features, similar to those in Figure 3E, are imaged on a number of the debris-flow surfaces (Fig. 5A).

Overridden moraine ridges. In the central part of the Negribreen submarine basin, on the eastern side, there is a further series of largely parallel, transverse ridges (Figs. 3D, 5A). The ridges are slightly sinuous in plan form and are up to 3 km long. They are on average 300 m wide with crests spaced about 400 m apart. The ridges are up to 15 m high and are generally parallel to the main moraine ridges further offshore. They are interpreted overridden retreat moraines from an earlier ice advance across the inner part of the submarine basin. Some of the ridges clearly show superimposed MSGLs, supporting this interpretation.

Medial moraine ridge. Towards the western edge of the submarine basin, a flow-parallel medial moraine is present (Figs. 2C, 5A). The ridge extends for 9 km, is 250 m wide and 40 m high ice-proximally and thins and decreases in height seawards; it can be traced almost to the inner of the two large moraine ridges on the western side of the submarine basin. The medial moraine is located at the transition zone between Negribreen and Petermannbreen, reflecting a time when they were further advanced and confluent, as shown in 1936 aerial photography (Fig.

5C). Negribreen has a drainage area an order of magnitude larger than that of Petermannbreen, so the latter was constrained between the larger Negribreen and the coastal hills to the west at that time.

Streamlined subglacial landforms. MSGLs, together with more widely spaced and sometimes attenuated linear features, form a slightly radial pattern in the central part of the submarine basin defined by the terminal moraines. They follow the main trend of the 80 to 150 m-deep trough. A 4 km-long field of drumlins is also present in the eastern part of the basin (Figs. 2B, 5A), about 3 km outside the present glacier front. Individual drumlins are blunt-nosed, about 1 km long and taper in an easterly direction. These are the only drumlins observed offshore of Olav V Land.

Small moraine ridges. The bulk of the area inshore of the large moraine ridges beyond Negribreen is covered by small moraine ridges, which are superimposed on underlying streamlined MSGLs and drumlins. These small ridges vary in orientation from transverse to parallel to former ice flow, suggesting an origin by annual still-stands/minor readvances or through deformable-sediment squeezing into basal crevasses. There are various transitional forms between these end members on the seafloor beyond Negribreen, yielding a boxwork or rhombohedral pattern in several places. Often, it has not been possible to separate between these small moraine types, and we therefore note the variability but map them simply as small moraine ridges. The ridges are generally just a few metres high, with a spacing of around 100 m.

Subglacial eskers and channels. Two eskers are observed in the inner part of the basin. Both begin just outside the modern glacier terminus where embayments are present associated with large turbid meltwater plumes. About 6 km seaward, the eskers merge and can be followed continuously for 1.5 km, with a further 1.5 km long fragment farther out. The general trend of the eskers is NNW-SSE. An additional esker merges with this system after 3 km. Maximum esker height is 25 m, but is generally less than 10 m high; the eskers are usually sinuous. Maximum width is 150 m, but is usually less than 100 m. Several small channels are also mapped in association with the eskers. Two of the channel systems are located upstream from the eskers in the deepest parts of the basin down to 140 m water depth. The largest channel is about 2 km long, 5 m deep and 50 m wide. Sometimes the channels enlarge to up to 7 m deep and 150 m wide. The channels are interpreted as elongate depressions eroded into subglacial sediments by meltwater under high pressure, continuing into depositional eskers when the channels instead cut upward into ice and eventually fill with debris as water flow wanes. On aerial photographs of the present tidewater glaciers the ice front is indented in several places (Fig. 5A). It appears that the subglacial drainage systems emerge preferentially at such indentations in the glacier terminus, which also coincide to some extent with the deepest water immediately offshore.

Unusual landform assemblage - Kvalrossøya. Kvalrossøya is now an island located about 10 km beyond the present (2011) front of Negribreen (Fig. 5A). This small island (1.2 by 0.3 km) of Triassic rocks has clearly functioned as an obstacle to ice flow during the surge of Negribreen in 1936. In the lee of the island, a distinctive suite of submarine glacial landforms was produced in a 3 km long and 1.5 km wide area (Fig. 5D). The landforms include glacial lineations developed on the large moraine ridges beyond, indicating that the lineations are slightly younger than the large ridge. 1936 aerial photographs show surface bands of dirty ice which have been deflected and folded around the then ice-covered Kvalrossøya (Fig. 5E).

4.2 Negribreen - recent glacier-margin fluctuations

Negribreen is the largest glacier system on Olav V Land, with a maximum flowline length of about 40 km and basin area 1,100 km^2 (Fig. 1) (Hagen et al., 1993). Its tidewater terminus is fed by several glaciers, of which Ordonannsbreen, Akademikerbreen and Opalbreen are the largest

(Fig. 1). The earliest recorded ice-front position for Negribreen comes from historical mapping from an 1870 expedition (Rabot, 1900; Lefauconnier and Hagen, 1991). Past locations of the ice front are also derived from Lefauconnier and Hagen (1991) (Fig. 5A), giving an indication of the behaviour of Negribreen over the last 140 years. The 1936 position is the most extensive (Fig. 5A), and the very crevassed nature of the glacier surface indicates that a surge was in progress at that time (Liestøl, 1969; Hagen et al., 1993). Since then, Negribreen has retreated continuously almost up to the present, by a maximum of about 20 km. Since July 2016 it has begun a new advance (T. Strozzi, pers. comm.).

The outermost large transverse moraine ridges identified about 12-20 km offshore of Negribreen (Fig. 5A) match clearly with the 1936 ice-front position derived from oblique aerial photographs (Lefauconnier and Hagen, 1991). A second pronounced ridge on the western side of the area appears to have formed during retreat of the ice front between 1936 and 1948, according to the map of Lefauconnier and Hagen (1991), and may represent a still-stand or even minor readvance of the terminus. The shape of the submarine area affected by the surge is thus about 25 km wide and up to 20 km long, with an area of 320 km^2. The inner bay exposed by subsequent ice retreat is up to 150 m deep, shallowing seaward and reaching 80-90 m in depth in the central part of the outer moraine ridge. The terminal moraine formed by this surge event marks the likely maximum extent of this glacier system during the Holocene, since the seafloor beyond appears largely smooth and fine-grained, and no other evidence of earlier, larger neoglacial fluctuations is present in the submarine landform record further offshore.

4.3 Helge Backlundbreen - submarine landforms

Multibeam swath-bathymetric data of the submarine glacial landforms offshore of Helge Backlundbreen, together with their mapped distribution, are shown in Figure 6. The area affected by recent glacier advance is the smallest of the nine submarine basins investigated and the variety of subglacial and ice marginal landforms observed here is also limited compared with the other areas mapped in this study.

Large transverse moraine ridges. The submarine basin inside a prominent and largely continuous terminal moraine ridge contains several relatively substantial ridge segments (Fig. 6A, B). The largest, outermost submarine ridge is 20 m high and 400 m wide. It is about 2 km long and can be clearly traced onto land on both sides, where it forms lateral moraines to modern Helge Backlundbreen (Fig. 6C). The distal slope of the terminal moraine shows no signs of instability and debris flowage. The relatively large moraine ridge in the middle of the basin appears to be overlain by small transverse moraine ridges implying that it is an older ridge, probably overridden by the 1936 surge.

Streamlined subglacial landforms. Just two possible glacial lineations, with a NNW-SSE direction, are observed on the southern side of the submarine basin. They are 400 m long, up to 3 m high, and sub-parallel to one another. Several small transverse ridges are superimposed on these features as is a larger moraine ridge segment. On land exposed by glacier retreat from its terminal moraines, several streamlined lineations are also present.

Small moraine ridges. About 15 smaller and discontinuous transverse-to-flow moraine ridges are mapped. They are generally 1 to 5 m high with an average spacing of around 50 m and a mean width of 20 m. These small ridges overlie the large transverse moraine ridge in the middle of the basin, indicating that they are younger and related to ice retreat after the 1936 surge.

Kettle holes. In the northern part of the submarine basin, close to the subaerial lateral moraine ridge, there is a 300 m diameter and 10 m deep depression, interpreted as a kettle hole (marked k in Fig. 6A). The bottom of the depression has a water depth of about 15 m. Several smaller depressions are also mapped (Fig. 6B).

4.4 Helge Backlundbreen - recent glacier-margin fluctuations

Helge Backlundbreen has an area of about 27 km^2 and a length of 9 km (Lefauconnier and Hagen, 1991), making it one of the smaller glaciers in Olav V Land. Its surface was also heavily crevassed in 1936, and looped lateral moraines on its western side also imply past surge activity (Fig. 6C) (Lefauconnier and Hagen, 1991). The glacier has retreated almost 2 km since 1936; this is a smaller terminus fluctuation than any of the other glaciers we discuss.

The well-defined large submarine ridge defines the recent maximum extent of Helge Backlundbreen (Fig. 6A), and the 1936 ice front is close to this location (Lefauconnier and Hagen, 1991). This, together with observation that the 1936 surface was crevassed, suggests a surge that began shortly before these oblique photographs were acquired. The exposed submarine basin is up to 2 km wide and a little more than 1 km long, with an area of about 2.5 km^2; the water is up to 30 m deep (Fig. 6). There is no evidence of earlier Holocene glacier fluctuations beyond the mapped terminal moraine ridge.

4.5 Sonklarbreen - submarine landforms

Submarine landforms beyond the present terminus of Sonklarbreen are shown in swath-bathymetric imagery (Fig. 7A) and are mapped in Figure 7B. A considerable variety of subglacial and ice marginal landforms is present; these landforms are described below.

Large transverse moraine ridges and debris-flow lobes. Two major moraine ridges are present, defining the limits of recent advances of Sonklarbeen (Figs 3A, 7A-B). The crest of the outermost ridge is a maximum of 10 m high and has a maximum width of 700 m. The multibeam bathymetric dataset does not cover the whole ridge, but the ridge is nonetheless estimated to have a total length of 18 km, including an exposed termino-lateral part in the far west (Fig. 7A). A second large moraine ridge, with two cresentic components, is present about 1 km inside the outermost ridge. It reaches a height of about 20 m, a width of 1.5 km and is about 15 km long. On the ice-distal flanks of each of these large ridges, a series of lobate features, interpreted as debris-flow lobes, is present (Fig. 7A). Five further moraine ridges of intermediate size are also mapped in the eastern part of the submarine forefield (Fig. 7A). They are up to 4 km long, 200 m wide and 10 m high with an average spacing of about 300 m.

Overridden moraine ridges. Several subdued ridges are present in the basin defined by the large outermost moraines of Sonklarbreen (Fig. 7A, B). These ridges are overprinted by both flow-parallel streamlined lineations and, subsequently, by small transverse-to-flow ridges. They probably formed during a previous surge of Sonklarbreen.

Streamlined subglacial landforms. Several glacial lineations (Fig. 2A) have been imaged on the sea floor beyond the modern terminus of Sonklarbreen (Fig. 7A). These generally follow the main axis of the trough and appear in a fan-shaped form likely parallel to the direction of past ice-flow (Fig. 7B). They reach a length of 1 km, and are generally up to a few metres high. These linear ridges, which are interpreted to have formed subglacially, are not so obvious as similar features in many of the other glacier forefields offshore of Olav V Land. This may be due to the many small transverse ridges superimposed upon them.

Small moraine ridges. Several sets of small ridges, interpreted as a combination of transverse-to-flow small retreat moraines (Fig. 3B) and more complex crevasse-fill ridges (Fig. 2D), have been mapped over a large part of the area inside the large moraines, especially in the east of the imaged area (Fig. 7A-B). Along a 2,100 m long transect here, we have mapped 40 ridges giving an average spacing between the individual ridges of about 50 m. The average width of the ridges is about 20 m and mean height is 2 m.

Subglacial eskers and channels. Three esker ridges and channel systems are identified and mapped in the inner part of the Sonklarbreen submarine basin within a kilometre or two of the modern ice front and close to indentations in the tidewater glacier terminus (Fig. 7A-B). Beyond the western indentation two esker systems are present (Figs. 2E, 7A). The first begins close to the present ice margin and extends 1,300 m south before turning southwest for a further 500 m. The esker is generally less than 50 m wide, but it extends into several fan-shaped forms where it is both higher and wider (150 m wide, 17 m high). The second western esker is 1,100 m long, with two ridge segments and a small linking channel between. It is up to 30 m wide and 2 m high. The linking channel is 100 m long and 1-2 m deep. A third esker system is developed outside an indentation in the eastern part of the present glacier front (Fig. 7A). It has a general NW-SE direction and is 1.6 km long. It begins as one ridge, dividing into two after 300 m with the smaller ridge continuing for 700 m. The main esker is 30-50 m wide and 5-10 m high. At about 1,000 m downflow it expands to a mound which is 20 m high and 150 m wide. Thereafter it narrows to 60-80 m in width and 5-10 m high. A small channel also exists about 200 m east of this esker system (Fig. 7A). It is parallel to the esker, 800 m long, 40 m wide and 3 m deep.

Kettle holes. In the westernmost part of the imaged area, a series of small depressions are developed in water depth of less than 40 m (mostly 10 to 25 m water depth) over an area of about 4 km^2 (Fig. 7A-B). They are oval to sub-rounded in planform and individual holes reach a depth of 10 m and an area of 200,000 m^2 (Fig 3F).

4.6 Sonklarbreen - recent glacier-margin fluctuations

Sonklarbreen has a 9 km-wide modern tidewater terminus, a maximum flowline length of 17 km, and is fed by a drainage basin of about 270 km^2 (Fig. 1) (Hagen et al., 1993). An early map drawn in 1870 provides the first observational information on this glacier (Heuglin, 1872). This historical position is close to the modern ice-front location in 2011 vertical aerial photographs (Fig. 7A). Reports from expeditions to the area in 1898 and 1900 suggested no unusual activity (Lefauconnier and Hagen, 1991). Given that the glacier extended about further 2-3 km seaward on 1936 oblique aerial photographs (Fig. 7C), it is likely that a surge occurred sometime during these 36 years. The lack of crevassing on 1936 photographs also suggests that a surge probably took place in the first decade or so of the 20th Century. Lefauconnier and Hagen (1991) also suggest that Sonklarbreen may have had an earlier maximum position indicated by prominent lateral moraines that also appear both in the early maps and on modern aerial photographs (Fig. 7A), implying that either an earlier surge or a Little Ice Age maximum position was attained sometime prior to 1870.

Both the position of the 1936 terminus of Sonklarbreen and the large terminal moraines observed in seafloor imagery (Figs. 7A, C) suggest that the ice front has retreated by about 10 km since their deposition. The formation of the terminal moraines almost certainly preceded 1936, as the glacier was clearly in the quiescent phase of the surge cycle by then, given the lack of surface crevassing (Fig. 7C). It is less clear whether the early 20th Century surge reached the outermost moraine ridge or halted at several large ridges about a kilometre further inshore (Fig. 7A). If the latter was the case, then the outermost large ridge represents either a pre-1870 surge or the Little Ice Age maximum response to the regional climatic cooling of the previous few centuries (e.g. Grove, 1988; Werner, 1993). The overall morphology of the 82 km^2 area inside these large moraines is that of a relatively simple 10 km wide and 10 km long submarine basin whose greatest water depth is 70 m at about 6 km from the modern ice front (Fig. 7A).

4.7 Pedasjenkobreen - submarine landforms

Multibeam swath-bathymetric data from offshore of Pedasjenkobreen and the mapped distribution of landforms are illustrated in Figure 8A-B. The observed submarine landform types are outlined below.

Large transverse moraine ridges. Several large transverse moraine ridges are mapped up to 4 km offshore of the modern margin of Pedasjenkobreen (Fig. 8A). The outermost terminal ridge is about 400 m wide, has a 10 to 20 m high crest and is about 2 km long. Further pronounced ridges are 300 to 400 m wide and 8 to 15 m high. There is little evidence of debris-flow lobes on the ice-distal flanks of the ridges.

Streamlined subglacial landforms. Well-developed glacial lineations have been imaged in the main inner basin (Fig. 8A). They are generally sub-parallel to the basin axis and cross-cut the innermost large moraine ridge (Fig. 8A-B). Individual lineations can be up to 1.5 km long, 1 to 2 m high and are spaced about 80 to 100 m apart, within the envelope of MSGL dimensions described by Spagnolo et al. (2014).

Small moraine ridges. In the main submarine basin defined by the large ridges, several small transverse-to-flow ridges are present (Fig. 8A-B). They are generally sub-parallel to the large moraine ridges, although occasionally they are more oblique. The small ridges are up to 5 m high, with an average spacing of 40 m. They probably represent both retreat moraines (when transverse-to-flow) and crevasse-fill ridges (when more obliquely orientated).

Subglacial eskers and channels. On the eastern, ice-proximal side of the inner submarine basin there is a channel and esker system of 2 km in length (Fig. 8A-B). Two small channels merge into one after 400 m and continue for 500 m, crossing the innermost large moraine ridge. The system then continues as an esker for 800 m. The channels are up to 1 m deep and 10 to 20 m wide, and the esker is up to 5 m high and 50 m wide. Given its clearly up-and-down long profile (Fig. 8A), the system must have been formed subglacially under high water pressure (e.g. Shreve, 1972).

Kettle holes. Several large, flat-floored depressions 5 to 10 m deep are present on the western side of the Pedasjenkobreen submarine basin in water depths of less than 15 m (Fig. 8A-B). There is evidence that the relatively steep walls defining these kettle holes have collapsed in some places, with small debris-flow lobes visible protruding into the depressions from the side walls.

4.8 Pedasjenkobreen - recent glacier-margin fluctuations

Pedasjenkobreen is about 39 km^2 in area and almost 9 km in length today (Hagen et al., 1993). Lefauconnier and Hagen (1991) reported, based on 1936 oblique aerial photographs showing the detailed morphology of subaerial lateral moraines, that the glacier had probably undergone three advances linked to surges and a possible Little Ice Age maximum position. Vasiliev's early map of 1900 shows the ice-front position in the embayment 1.5 km inside the curved subaerial lateral-moraine ridge, not far from its modern position on 2011 imagery (Fig. 8A). It is clear from 1936 oblique photography that the glacier had advanced at least to the ice-proximal flank of the prominent subaerial lateral moraine ridge at that time (Fig. 8C). In addition, its terminus was still crevassed, indicating surge activity at or shortly before 1936.

The seafloor morphology off modern Pedasjenkobreen consists of a 5 km^2 area that reaches no more than about 30 m in water depth (Fig. 8A), bounded by three prominent submarine moraine ridges. The ridges are presumably the underwater equivalents of the detailed crest morphology within the subaerial lateral moraine. At least the innermost of these three large ridges is a product of glacier surging, marking the limit of the 1930s or slightly earlier surge activity. The more ice-distal ridges may represent previous surges and, possibly, the Little Ice Age glacial limit.

4.9 Besselsbreen – submarine landforms

Multibeam bathymetric imagery of the submarine glacial landforms offshore of the present terminus of Besselsbreen is shown in Figure 9A. The distribution of these landforms is mapped in Figure 9B and discussed below.

Large transverse moraine ridges and debris-flow lobes. A major moraine ridge, with two arcuate components, defines the recent outer limit of Besselsbreen (Fig. 9A). The ridge crest, of maximum width 1,500 m and height of about 20 m, is at up to 45 m in water depth. Along its outer flanks a series of coalescing debris-flow lobes is present. The transition from ice-distal moraine flanks to debris-flow deposits begins at a water depth of around 40-50 m and ends on the sea bottom between 55 and 70 m.

Medial moraine ridge. A medial-moraine ridge (Fig. 2C) separates the eastern and western parts of the submarine basin defined by the major terminal moraine (Fig. 9A). This feature does not appear to be linked to the subaerial medial moraine that divides ice of Besselsbreen from the neighbouring Augnebreen (Fig. 9A), or that on the 1936 ice surface, which is presumably displaced well to the east by an earlier advance of Besselsbreen (Fig. 9C).

Streamlined subglacial landforms. Some sub-parallel glacial lineations have been mapped on the floor of the submarine basin (Fig. 9A). They follow the main trend of the two trough axes (NNW-SSE). Individual streamlined lineations are up to 3 km long and less than 5 m high. They are overprinted and partially obscured in many places by smaller ridges (Fig. 9B).

Small moraine ridges. Large numbers of small moraine ridges have been mapped inside both the eastern and western submarine basins (Figs. 2D, 3B, 9A). The ridges clearly overlie the glacial lineations (Figs. 2D, 9A). In the eastern basin there is a well-developed pattern of small retreat moraines (Fig. 9A). About 25 ridges are mapped along a 2.5 km long transect giving an average spacing of approximately 100 m. Average ridge width and height are about 60 m and 4 m (max. 10 m), respectively. However, in the western basin in particular it is difficult to decide if these features are transverse-to-flow retreat moraines or more complex rhombohedral crevasse-filled ridges. Where a clear boxwork structure is identified (Figs. 2D, 9A), individual ridges are generally smaller than the retreat moraines; for instance, in one area we have measured an average ridge width and height of 30 m and 3 m, respectively.

Eskers and channels. In the inner western basin two eskers are present (Fig. 9A, B). The westernmost is about 2 km long, 10 m high and 100 m wide, with a S-N orientation. The more easterly and larger esker is nearly 7 km long, and is also orientated S-N. It is composed of at least four parts, up to 15 m high and 100 m wide. In the inner eastern basin there are several channels with a SSW-NNE orientation (Fig. 9A, B); the longest is 2 km. Each is relatively straight, about 2 m deep, with a width of less than 50 m.

Kettle holes. In the ice-proximal part of the eastern basin beyond modern Besselsbreen, several kettle holes are mapped in water less than 35 m deep (Fig. 9A). The two largest are sub-circular, 500,000 m^2 and 300,000 m^2 in area and up to 10 m deep with steep sides and flat floors.

4.10 Besselsbreen - recent glacier-margin fluctuations

Besselsbreen drains northwards from the 600 km^2 ice cap on Barentsøya (Dowdeswell and Bamber, 1995), and is almost 150 km^2 in area with a maximum length of 22 km. The earliest evidence for the ice-front position of Besselsbreen is from oblique air photographs acquired in 1936 (Fig. 9C). At that time the glacier was protruding well beyond the line of the coast to the east, but constrained along its western shoreline. Its surface appears uncrevassed and with a very low gradient (Fig. 9C). In addition, a number of tabular icebergs are imaged, suggesting that the terminus region may have been temporarily afloat due to thinning (Dowdeswell, 1989). Since that time, Besselsbreen has retreated about 5 km to its present location, still in tidewater but now in a coastal embayment (Fig. 9A).

The submarine morphology shows a 10.5 km wide and 11 km long depression, of about 81 km^2, bounded by a large arcuate terminal ridge (Fig. 9A). A subdued medial moraine divides the 60 m deep western basin from the 50 m deep eastern basin. There is no direct evidence of a past surge of Besselsbreen or the neighbouring Augnebreen (Lefauconnier and Hagen, 1991), but it is clear that the large moraine ridges mark either the surge limit or that of the Little Ice Age maximum position, from which the glacier terminus has retreated about 10 km to its modern location. In addition, the presence of many rhombohedral crevasse-fill ridges indicates strong basal crevassing suggestive of past surge activity (e.g. Solheim, 1985; Dowdeswell et al., 2016a)

4.11 Hannbreen – submarine landforms

Multibeam bathymetry from beyond the modern margin of Hannbreen is shown in Figure 10A. The mapping of landforms in Figure 10B is impeded by a drape of apparently fine-grained and probably current-delivered sediment, especially within a kilometre of the coastline, which has at least partly buried many of the finer-scale glacial landforms beyond Hannbreen; it is the only one of the 9 areas we have studied that shows this characteristic (Fig. 4B). The identifiable landforms are discussed below.

Large transverse moraine ridges. A major arcuate moraine ridge defines the maximum recent position of the glacier terminus (Fig. 10A). The ridge crest is in a maximum of 25 m water depth and reaches a maximum width of 700 m and height of about 10 m. It is indented at about 7 points on its ice-proximal side, perhaps reflecting variations in marginal ice thickness and the time of furthest advance. At least five additional moraine ridges have been mapped nearer to the modern coastline; they are up to 300 m wide and a few metres high. No debris-flow lobes are identified on the distal flanks of any of the ridges.

Streamlined subglacial landforms. Well-developed sets of glacial lineations have been mapped in the Hannbreen submarine basin (Fig. 10A). They form an overall fan-shaped pattern (Fig. 10B). Individual MSGLs are up to 1 km long, from a few to 7 metres high and spaced about 100 to 150 m apart. They overprint several of the larger transverse ridges, before some details of the seafloor topography become obscured by draping sediments close to the coast.

Small moraine ridges. A few small moraine ridges have been mapped in the central part of the outer submarine basin, sometimes superimposed on the lineations (Fig. 10A-B). The ridges are either parallel with or transverse to past glacier-flow direction (W-E). Several transverse-to-flow ridges are mapped just inside the terminal moraine ridge; they have average spacing of about 40 m and a width and height of 20 m and 2 m, respectively. By contrast, in the central part of the submarine basin, small ridges of similar dimensions are orientated sub-parallel to past ice-flow (Fig. 10A). These ridges are probably crevasse-fill ridges. In the inner basin, much of the seafloor has a subdued appearance, with some landforms clearly being buried by a sedimentary drape. Sometimes only the upper parts of small ridges remain above what is presumably a fine-grained fill (Fig. 4B) that is probably being deposited from longshore currents before they enter the narrow Heleysundet between eastern Spitsbergen and Barentsøya (Fig. 1). There is much evidence of current transport and reworking of fine-grained sediment to the west of Heleysundet (Fig. 4C-D). The generally NE-SW orientation of iceberg ploughmarks offshore of Hannbreen (Fig. 10A), indicating the general direction of iceberg drift, also supports this interpretation.

4.12 Hannbreen - recent glacier-margin fluctuations

Hannbreen drains eastwards from the Olav V Land ice cap and today terminates at the coast with only a 400 m-wide section of the glacier terminus reaching the sea (Fig. 10A). Its area is about 40 km^2 and it has a length of 13 km (Lefauconnier and Hagen, 1991). No observations are available prior to 1936 oblique photographs, which show a large lobe protruding into open water well beyond the coastline (Fig. 10C). Hannbreen's surface is relatively uncrevassed but has looped moraines, providing indirect evidence of a past surge (Meier and Post, 1969). Lefauconnier and Hagen (1991) speculate that the glacier had reached a surge maximum position a few years before 1936. Since 1936, the glacier front has retreated about 2.5 km to reveal many of the submarine landforms that are mapped in Figure 10B.

The large terminal moraine ridge identifies the maximum extent of the early 20th Century surge of Hannbreen (Fig. 10C). The 15 km^2 basin defined by this ridge is about 4.5 km wide and 4.5 km long with a maximum water depth of about 30 m. The 1936 position of the ice front is about 2 km inside the terminal moraine ridge, although it may be that Lefauconnier and Hagen have slightly underestimated the extent of the 1936 ice front.

4.13 Koristkabreen – submarine landforms

Multibeam swath-bathymetry offshore of Koristkabreen is illustrated in Figure 11A, with distribution of submarine landforms shown in Figure 11B and discussed below.

Large transverse moraine ridges and debris-flow lobes. A single main terminal moraine ridge defines the submarine basin adjacent to the modern margin of Koristkabreen (Fig. 11A). Prominent subaerial lateral moraines on either side of Koristkabreen clearly correlate with the submarine terminal moraine (Fig. 11A). The terminal ridge appears to be indented on its ice-proximal side by at least eight individual features, which may relate to fingers of a broken or notched ice margin during its last advance; there is some limited evidence for this in 1936 aerial photographs (Fig. 11C), although the recent maximum glacier position was to seaward of the photographed location. The ridge crest is in water depths between 10 and 60 m and reaches a maximum height of about 20 m; some of the indentations in the ridge mean that it is less well developed and is only a few metres high and 300 to 800 m wide in some places (Fig. 11A). The outer flank of the moraine ridge translates into a number of well-defined debris-flow lobes along most of its perimeter (Figs. 3E, 11A). The largest debris-flow lobe is 1,300 m wide and extends over 2 km beyond the moraine ridge reaching a water depth of 125 m. The cross-cutting relationships between debris-flow lobes suggest at least three superimposed lobes, with thicknesses up to about 10 m.

Streamlined subglacial landforms. Well-developed sets of glacial lineations with a radial or fan-shaped pattern have been mapped on the sea floor of the Koristkabreen submarine basin (Figs. 2A, 11A). These tend to follow the pattern of indentations visible in the detailed morphology of the terminal moraine and may relate to fingers of ice where they impinged upon the ice-proximal side of the ridge. They cover most of the length of the basin, with ridges a few metres high and 40 m wide, spaced about 50 m apart. Some of the streamlined features appear to begin from slightly blunt-nose drumlinoid features, implying a position on the continuum of lineations between drumlins and MSGLs (Fig. 2A).

Small moraine ridges. A series of small transverse-to-flow retreat moraines is superimposed on the glacial lineations (Fig. 11A). Up to 30 ridges are mapped along a 1.2 km long transect, giving an average spacing of 40 m. The ridges are up to 400 m long, up to 50 m wide and 1 to 3 m high. No signs of subglacial meltwater channels or eskers are observed in the Koristkabreen submarine basin.

4.14 Unnamed glacier west of Koristkabreen (Kw) – submarine landforms

The submarine landforms seaward of the unnamed glacier are also shown in Figure 11A; their distribution is mapped in Figure 11B and outlined below.

Large transverse moraine ridges and debris-flow lobes. The outermost moraine ridge is located 3 km beyond the present (2011) ice margin of this glacier; the ridge is up to 20 m high and a few hundred metres wide (Fig. 11A). The unnamed glacier also has subaerial lateral moraines on both sides, the eastern one of which clearly correlates with the terminal submarine ridge (Fig. 11A). On the distal side of this terminal ridge several well-developed debris-flow lobes are present; the largest is 2 km wide and 1 km long and ends in 80-90 m water depth. Some debris flows superimpose on one another, although this is not so well developed as in front of the neighbouring Koristkabreen. In addition, there are two sub-parallel finger-like features composed of linear ridges with small orthogonal transverse ridges between them that protrude over a kilometre beyond the outermost moraine ridge (Fig. 11A). These may represent tongues of ice which impinged on the sea floor when the unnamed glacier was at its recent maximum position. It appears as though the terminal moraine ridge of Koristkabreen superimposes on the eastern side of the unnamed glacier terminal moraine (Fig. 11A), implying that the advance of Koristkabreen took place after that of the unnamed glacier. A further transverse ridge is present across the whole basin about 1 km from the modern ice front with debris-flow lobes up to 1.6 km wide and 0.7 km long on its ice-distal flanks. This represents either a later still-stand or a subsequent readvance of the terminus of the unnamed glacier.

Streamlined subglacial landforms. Well-developed sets of glacial lineations with a radial pattern are found in the main submarine basin offshore of the unnamed glacier (Fig. 11A-B). Most of the lineations are found outside the large inner moraine, but a few are also found close to the present ice margin. The individual ridges are up to 1500 m long, 10 m high and a few hundred metres wide.

Small moraine ridges. A series of small transverse ridges is superimposed on the glacial lineations in the outer part of the submarine basin. These ridges are generally small, up to a metre high and 20 m wide with an average spacing of around 35 m. Their lack of complexity suggests that they are more likely to have been formed at a retreating ice margin than by squeezing of sediment into basal crevasses.

Kettle holes. Several flat-floored depressions, with clearly defined rims define kettle holes on both sides of the submarine basin; kettle holes up to 15 m deep occur in water no more than 25 m deep (Fig. 11A).

4.15 Koristkabreen and adjacent unnamed glacier - recent glacier-margin fluctuations

Koristkabreen has an area of about 50 km^2 and is approximately 13 km long (Lefauconnier and Hagen, 1991). The unnamed glacier, 5 km to the northwest, has a slightly larger drainage basin of about 68 km^2 but a shorter length of about 10 km. Both glaciers now have tidewater ice fronts that terminate in embayments in the coast (Fig. 11A). The first observations of these two glaciers are from 1936 oblique aerial photographs. These images show both glaciers with lobate ice fronts protruding beyond the general line of the coast, but with uncrevassed surfaces. There has been no observed surge of either glacier (Lefauconnier and Hagen, 1991), and the uncrevassed surfaces in 1936 photographs imply that, if a surge was responsible for their advances, then these events probably happened several decades earlier.

Comparing the 1936 position of each glacier with the offshore bathymetry shows that both glaciers were about 1.5 km inside the terminal ridge marking the outer limit of recent ice advance

(Fig. 11A-C). The total retreat since this maximum has been 4 km for Koristkabreen and about 2.5 km for the adjacent unnamed glacier. This retreat has exposed submarine basins of 11 and 7.5 km^2 which reach maximum depths of 60 and 50 m for Koristkabreen and the unnamed glacier, respectively.

4.16 Hochstetterbreen – submarine landforms

Multibeam swath-bathymetric data imaging the glacial landforms offshore of Hochstetterbreen, together with their interpreted distribution pattern, are illustrated in Figure 12A-B. This is the northernmost glacier in our study and also has the second largest drainage basin (Fig. 1).

Large transverse moraine ridges and debris-flow lobes. Several large moraine ridges are present, with the outermost ridge defining the limit of recent ice advance across the Hochstetterbreen submarine basin (Fig. 12A). This outermost, and largest moraine ridge is 22 km long and 1 to 2 km wide, narrowing to about 500 m at its western end; it has several distinctive elements, representing the irregular shape of the advancing ice terminus. The ice-proximal side of the ridge has several subdued indentations, which are less conspicuous than those in terminal moraines offshore of Hannbreen and Koristkabreen in particular (Figs. 10A, 11A). The maximum distance from the present ice front to the northeastern part of the terminal ridge is 14 km. The water depth of the ridge crest varies between 35 and 70 m and reaches up to of 30 m above the surrounding seafloor. Debris-flow lobes up to 2 km wide and 0.7 km long extend from the ice-distal side of the ridge into water about 80 m deep (Fig. 12A). A second ridge complex, containing two crests, is located up to 2 km behind the terminal moraine and has a length of 9 km and a width of 200-300 m (Fig. 12A-B). Several less well-defined ridges are also present in the inner submarine basin, one appearing to link with lateral moraines onshore (Fig. 12A).

Streamlined subglacial landforms. A series of subglacial lineations are present and have a fan-like pattern, opening out with increasing distance from the present ice margin (Fig. 12A). Individual lineation ridges may reach a length of 3 km. The lineations are a few metres high and the average spacing is 150 m. They cross-cut some of the less well-defined but relatively large transverse moraine ridges in the mid and inner Hochstetterbreen submarine basin (Fig. 12A-B).

Small moraine ridges. A limited number of small transverse-to-flow retreat ridges are present in the innermost part of the submarine basin. They are superimposed on the subglacial lineations, representing retreat of the ice margin. The transverse ridges are up to 300 m long, up to 50 m wide and a few metres high.

4.17 Hochstetterbreen - recent glacier-margin fluctuations

Hochstetterbreen is one of the larger glaciers draining the Olav V Land ice cap, at about 580 km^2 and 37 km long (Lefauconnier and Hagen, 1991). Historical mapping by de Geer showed that the glacier protruded 5-7 km beyond the coastline in 1901. De Geer also mentioned in this report a map of 1868 by Koldewey that placed the ice front at the coastline, implying a rapid advance, likely a surge sometime during this 33-year interval (Lefauconnier and Hagen, 1991). By 1936, Hochstetterbreen had retreated back to the coastline and the view offered by oblique aerial photographs shows a crenulated ice front and a largely uncrevassed ice surface, suggestive of post-surge stagnation and retreat (Fig. 12C). Retreat has continued since the 1930s, and today the 11 km-wide tidewater ice front is about 4 km inside the general coastline (Fig. 12A).

The large, outermost moraine ridge, with several debris-flow lobes beyond it, is clearly visible in the bathymetry of the offshore area (Fig. 12A). This well-defined terminal moraine is similar in general form to the mapping of de Geer, which was undertaken from Wilhelmøya, several kilometres to the north (Fig. 1). Only a small northward shift in the position of the 1901 margin reproduced in Lefauconnier and Hagen (1991) would provide an almost exact match with the location of the submarine terminal moraine. This implies that the surge of Hochstetterbreen may have taken place only a short time before 1901. The submarine basin, of 75 km^2 in area and maximum depth 120 m, revealed by ice retreat since that time is about 6 km wide close to land, widening to about 10 km farther offshore (Fig. 12A).

5. Submarine Glacial Landform Distribution in an Open-Marine Setting

The distribution of submarine glacial landforms in the open-marine setting of eastern Svalbard is shown in Figure 13. The occurrence of individual landform types is listed in Table 1. The seafloor imaged adjacent to the nine eastern Svalbard glaciers has several general characteristics.

Each glacier has a large submarine terminal moraine, or set of terminal ridges. Inside these large ridges is a submarine basin or basins of varying depth that has been exposed by tidewater glacier retreat over the last approximately 80 to about 150 years (Fig. 13), according to aerial photographic and earlier historical evidence (e.g. Heuglin, 1872; Nordenskiöld, 1875; Rabot, 1900; Liestøl, 1969; Schytt, 1969; Lefauconnier and Hagen, 1991). The terminal ridges represent the furthest recent advance of each glacier and demonstrate that all of them have expanded out from the general line of the coast as lobes into open water for part of this period (Fig. 13). The ridge crests generally exhibit ploughing by iceberg keels (e.g. Fig. 10A). On the distal flanks of the terminal ridges, soft sediment failure has, in six of the nine cases (Table 1), produced a series of overlapping debris-flow lobes (e.g. Figs. 3E, 13). The material involved in debris flowage may, in part at least, be supplied by advection of deforming subglacial till during the active phase of the surge cycle, together with slope failure on distal moraine ridge flanks. Clearly defined debris-flow lobes are absent from beyond Helge Backlundbreen, Pedasjenkobreen and Hannbreen, which are also the glaciers with the smallest drainage basins (Table 1). We note that debris-flow development is very sensitive to both local slope angle and sediment clay/water content – for the latter we have no relevant observations.

Inshore of the terminal ridges of each glacier there is a well-preserved and clearly visible set of glacier-influenced submarine landforms, with the detailed components varying between individual glaciers (Fig. 13). The main exception to this is Hannbreen, where it appears that the inner part of the submarine landform assemblage is being progressively buried by draping sediments (Figs. 4B, 10A). The seafloor in the northwestern part of the submarine basin beyond Besselsbreen is also affected to a lesser extent by sediment draping (Fig. 9A). The draping is probably a function of strong tidal-current activity and associated sediment transport and deposition in this area, close to the topographic constriction of Heleysundet, a narrow channel linking Storfjorden and the Northwest Barents Sea (Fig. 1). Here, *Den Norske Los* (the Norwegian pilot or navigation guide) warns mariners of possible current speeds of 8-9 kts. Southwest of Heleysundet, the presence of mounded drift deposits, about 2 km long and up to 700 m wide and 15 m high (volume about 0.2 km^3), and trains of current ripples <50 cm high and spaced 10 to 15 m apart with the same orientation, support this interpretation (Fig. 4C-D).

The occurrence of each individual landform type in the exposed basin or basins between each modern glacier terminus and the prominent submarine terminal moraines is set out in Table 1; landforms include terminal ridges and associated debris-flow lobes, streamlined glacial lineations (MSGLs, drumlins and the continuum of streamlined landforms between them), eskers/channels, small traverse-to-flow and more complex boxwork ridges, and kettle holes. There are also several medial moraines (Fig. 2C). It is clear that the vast majority of submarine basins contain most of the individual landforms described earlier, each of which has been associated previously with phases of the glacier surge cycle (e.g. Solheim, 1991; Ottesen and Dowdeswell, 2006; Ottesen et al., 2008; Flink et al., 2015; Dowdeswell and Ottesen, 2016b). The most obvious exception to this is the submarine basin of Helge Backlundbreen (Fig. 6), where evidence of debris-flow lobes, crevasse-fill ridges and channelized water flow is lacking and streamlined lineations indicative of past rapid flow are very limited except on subaerially exposed land (Figs. 6A, 13; Table 1).

More generally, erosional and depositional evidence of subglacial water flow is also present in the submarine basins beyond four of the nine glaciers, including the relatively large Negribreen, Sonklarbreen and Besselsbreen systems (Table 1). Previous observations of submarine landforms in Spitsbergen fjords where glacier surging has taken place have also shown that eskers and channels are not always present (e.g. Borebreen and Wahlenbergbreen, Ottesen and Dowdeswell, 2006; Tunabreen, Flink et al., 2015; Blomstrandbreen, Burton et al., 2016). Where eskers and channels are observed, it is often in association with major indentations in, and relatively deep-water areas beyond, modern ice margins (e.g. Nathorstbreen and Paulabreen, Ottesen et al., 2008). This is a similar morphological setting to the coincidence of major terminus indentations and channel/esker systems today close to the margins of Negribreen, Sonklarbreen and Besselsbreen (Figs. 5A, 7A, 9A).

The presence of submarine crater-like kettle holes has not been identified previously in the context of tidewater surge-type glaciers in Svalbard (Fig. 3F), yet is observed beyond six glaciers in the eastern Svalbard study area (Fig. 13, Table 1). Further, many subaerially exposed kettle holes are present on land affected by surges of Nathorstbreen and Paulabreen in western Spitsbergen fjords (Rowan et al., 1982; Ottesen et al., 2008), presumably linked to ice stagnation and melt. Given that glacier ice stagnates, especially early in the quiescent phase between surges, it is not surprising that such features are produced when the moribund ice melts and/or floats away to leave steep-sided submarine depressions. Once formed, infilling by fine-grained glacimarine sedimentation contributes to a smooth kettle hole floor, and side-wall collapse also provides infilling by debris flows. The kettle holes observed in eastern Svalbard, typically close to the lateral margins of submarine basins, are found in very shallow water often less than 20 m deep. Buoyancy considerations in deeper water would probably enable rapid lift-off and disintegration of stagnant ice, and this is likely why kettle holes are not found in relatively deep fjord waters in western Spitsbergen (e.g. Ottesen et al., 2008; Flink et al., 2015).

Further offshore in the eastern Svalbard study area, beyond the terminal moraine ridges, the seafloor is relatively smooth, with features such as bedrock ridges and knolls clearly being buried beneath a sediment drape. This suggests continuing sedimentation from rain-out of fine grained and probably glacier-derived debris over a long period. These distal glacimarine sediments are disturbed to varying degrees by iceberg grounding pits and ploughmarks (Fig. 4A), with the intensity of reworking depending on water depth and iceberg flux and drift tracks. There is little indication of earlier Holocene neoglacial ice advances seaward of the terminal moraine systems we have described for each of the nine glaciers. Indeed, it is likely that the streamlined MSGLs present in the centre of Ginevrabotnen, the 25 km-wide bay between Olav V Land and Barentsøya (Fig. 13), are an indicator of the direction of full or deglacial ice flow from the Last Glacial Maximum ice sheet on Svalbard and the Barents Sea (Svendsen et al., 2004; Hughes et al., 2016). Their NE-SW orientation is clearly unconnected to any recent glacier fluctuations.

6. Open-Marine Glacial Landform Assemblage and a Simple Schematic Model

6.1 Landform assemblage for glacier surges in open-marine settings

Although the distribution and frequency of occurrence of individual submarine landforms varies between each glacier, a general geomorphological pattern or landform assemblage emerges (Fig. 14, Table 1). In plan-view, the terminal moraines marking the limits of surge or Little Ice

Age advance usually have a distinctive lobate or arcuate form when, in open-marine settings, they are unconstrained by fjord walls. The Hannbreen, Koristkabreen and Hochstetterbreen submarine landform assemblages are clear examples (Figs. 10A, 11A, 12A). The submarine basin or sub-basins exposed inside these outer moraine ridges when ice retreats during the quiescent phase of the surge cycle, or due to post-Little Ice Age warming, contain a further suite of landforms. Typically the assemblage of landforms consists of several individual features, which are considered below in order of timing of deposition and stratigraphic superposition.

(a) Streamlined sedimentary landforms are produced during fast glacier flow in the active phase of the surge cycle when ice advances in an offshore direction. These streamlined glacial landforms, in the form of (i) MSGLs and other streamlined lineations, and occasionally (ii) drumlins (Fig. 2A-B), also indicate the direction of past ice flow; this is often fan-shaped as surging ice spreads out in an open-marine setting. (iii) Sometimes the lineations are superimposed on older sets of ridges within a submarine basin, which are inferred to be overridden relicts of terminal moraines marking the maximum position of past surges (Fig. 3D). Such buried and overridden ridges therefore represent, where present and identifiable, the oldest component of this landform assemblage.

(b) (i) Relatively large terminal ridges or sets of ridges define the maximum limit of ice advance, linked to surging or a Little Ice Age maximum (Fig. 3A). Two features may be associated with these relatively large moraines. (ii) Debris-flow lobes may be present on ice-distal moraine flanks associated with the failure of the deforming sediments that, under high water pressure, enable fast-flow and surging to take place (Fig. 3E). (iii) Indentations are sometimes seen on the ice-proximal terminal moraine flanks, probably linked to fingers of ice within the advancing glacier terminus (Fig. 3C).

(c) Small ridges, just a few metres high and space 50 to 150 m apart, that are either (i) relatively linear and orientated transverse-to-flow (Fig. 3B) or (ii) more complex and rhomboherdral or boxwork in pattern (Fig. 2D). It is sometimes difficult to distinguish between these two types of small ridge, but in general the complex boxwork moraines are more common closer to terminal moraines, whereas geometrically simpler transverse-to-flow moraines become more prevalent in inner-basin locations closer to the modern ice margin. This makes sense, given that the more complex ridges are interpreted to be a result of squeezing of soft subglacial sediments into basal crevasses shortly after the active phase of the surge cycle ceases, whereas small transverse ridges are linked to minor winter ice readvances of a grounded tidewater glacier terminus, which will take place as the quiescent phase proceeds.

(d) Esker and channel systems, produced by water flow in subglacial conduits, formed after an organized and relatively efficient hydrological system is re-established at the end of the active phase of a surge (e.g. Kamb et al., 1985). Several clear examples of drainage systems are present in the submarine basins beyond Negribreen and Sonklarbeen in particular (Fig. 2E-F; Table 1).

(e) Submarine kettle holes, sedimentary crater-like forms in shallow water usually at the lateral margins of submarine basins, left when stagnant ice melts and/or floats away as the glacier terminus retreats during the quiescent phase of a surge. The basin beyond Sonklarbreen has a number of well-developed examples (Fig. 3F).

6.2 Schematic model for glacier surges in open-marine settings

A new schematic model of the landform assemblage associated with tidewater glaciers surging into open-marine settings is set out in Figure 14. The broad-scale arcuate terminal moraines marking the surge outer limit provide a distinctive component of the geometry. These terminal moraines define a submarine basin or basins inshore, in which the remaining individual landforms typical of the nine glaciers investigated are located. The individual landforms making up the assemblage are labeled in terms of their timing of deposition within a surge cycle, from overridden ridges of a previous surge through to transverse-to-flow small ridges often deposited annually during terminus retreat during the quiescent phase of the cycle as ice retreats through the submarine basin (Fig. 14). It should be noted that not all individual landforms in the schematic model are necessarily present in association with a specific surge event; this is implied by the absence of some features from the submarine basins of some of the nine glaciers (Table 1).

This new schematic model of an open-marine surge-type landform assemblage can be compared with earlier models that were based on submarine landforms associated with surges in Spitsbergen fjords (Ottesen and Dowdeswell, 2006; Ottesen et al., 2008; Flink et al., 2015). The model of Flink et al. (2015) includes the terminal moraines and related debris-flow lobes of several surges of Tunabreen. We also see similar sequences of terminal ridges and associated debris flows in the submarine basins offshore of Negribreen and Sonklarbeen in particular (Figs. 5A-B, 7A-B). While there are many similarities, our model differs from existing landsystem models of surges into Svalbard fjords in several ways. First, the overall shape of the open-marine surging landsystem is arcuate, reflecting the lack of constraining fjord walls on overall morphology. Secondly, the ice-proximal sides of terminal moraine ridges are often indented, reflecting the sometime irregular and broken termini of tidewater glaciers surging into open water. Thirdly, the distribution pattern of streamlined lineations is generally fan-shaped, again reflecting either the lack of constraint by valley walls as an advancing ice front moves beyond the coastline or simply that a single drainage basin surges within a parent ice cap with a long length of terminal ice cliffs. Fourthly, we have observed crater-like depressions or kettle holes at the inner lateral margins of many submarine basins, linked to ice stagnation in shallow water. In addition, the presence of systems of eskers and channels is also prominent close to relatively deep water associated with indentations in the retreating ice front.

Our new schematic model relating to surges in open-marine settings, and earlier work on fjord landforms, have several elements in common with models of surging glacier landforms in terrestrial environments, but there are also some differences (Ottesen et al., 2008). A plan-form model of landforms in the forefield of an Icelandic surge-type glacier was given in Sharp (1985a). The observed landforms included surge-terminal ridges of glacitectonically thrusted sediments, and, closer to the modern glacier termini, chaotic hummocky topography, fluted till and crevasse-fill ridges. Evans and Rea (2003) presented a more detailed surging glacier landsystem model, based on terrestrial observations in Svalbard and Iceland. The model included thrust-block moraine, hummocky moraine, flutings and crevasse-squeeze ridges. Thrust-block moraines found at terrestrial surge margins are probably similar to multiple-crested submarine terminal moraines, such as those on the large eastern ridge offshore of Negribreen (Fig. 5A). Crevasse-fill ridges clearly occur in both terrestrial and marine settings (Fig. 2D). Hummocky moraines are widespread inside surge limits on land, but are absent on both fjord and open-marine sea floors. Ottesen et al. (2008) speculated that such hummocky topography might be a degraded form of the small rhombohedral and transverse-to-flow ridges observed in marine settings. Flutes in the model of Evans and Rea are somewhat similar in form, if not in scale, to MSGLs and other streamlined lineations from Svalbard marine sediments. Eskers have also been mapped from the forefields of Icelandic surge-type glaciers, formed by supraglacial or englacial streams guided by crevasse networks (Evans and Rea, 2003).

A final major difference between terrestrial and marine surge landsystems is that retreat moraines, often demonstrably annual, are widespread on the Svalbard sea floor inside surge limits (Fig. 3B), whereas they are absent in terrestrial settings. Ottesen et al. (2008) suggested that this may reflect different mechanisms of glacier wastage during the quiescent phase of the surge cycle. On land, glacier margins stagnate *in situ* following surge termination as glacier ice. At marine glacier margins, retreat is often by iceberg calving, which in Svalbard is most active during the summer months when sea ice is absent (Vieli et al., 2002). Ice-marginal moraines will form in winter when calving is suppressed, either by bulldozing if there is some basal motion, or by squeeze if the glacier ice is stationary.

Submarine geomorphic observational data are particularly useful in constructing landform assemblage models because of the lack of landscape modification after initial deposition at former glacier beds. This contrasts with the much more fragmentary and often reworked record provided by glaciers ending on land (Evans and Rea, 2004). The retreat of tidewater glaciers, whether of surge type or otherwise, is likely to take place mainly by mass loss through iceberg calving and occasionally by stagnation and melting in very shallow water – kettle holes are evidence of the latter situation. Submarine landforms are, therefore, less likely to be subject to the meltwater and debris-flow reworking processes that are very common at the retreating margins of glaciers ending on land (e.g. Lawson, 1979). In addition, the submarine landforms imaged in the seas around Svalbard are also observable at or close to the sea floor because sedimentation rates here are relatively low, at a few millimeters to tens of millimeters per year (e.g. Elverhøi et al., 1983; Dowdeswell et al., 1998). By contrast, in the fjords of southeast Alaska for example, sedimentation rates are two or three orders of magnitude higher (e.g. Powell and Molnia, 1989; Cowan et al., 2010) and any glacier-related landforms exposed at the sea floor by tidewater glacier retreat will be buried rapidly.

7. Links to Glacier Surging

7.1 Historical behavior of the eastern Svalbard glaciers

Fluctuations of the nine eastern Svalbard glaciers studied have been reconstructed from early maps and sketches and, more recently, from 1936 oblique aerial photographs followed by vertical aerial photographs and satellite images (Lefauconnier and Hagen, 1991). The observed fluctuations of each glacier, illustrated in Figure 15, provide an indication of whether surging has taken place in the past 150 years or so that is independent of the marine-geomorphic record. Our multibeam-derived location of the maximum recent position of each ice front is also shown (Fig. 15).

Negribreen is clearly a surge-type glacier; indeed its surge, which was observed in 1936 photographs (Fig. 5E), is among the largest recorded in Svalbard (Liestøl, 1969; Schytt, 1969). A new surge of Negribreen appears to have begun from July 2016 (T. Strozzi, pers. comm.). Five other glaciers, Helge Backlundbreen, Sonklarbreen, Pedasjenkobreen, Hannbreen and Hochstetterbreen, are also very likely to have surged in the decades before 1936 (Fig. 15), based on a combination of their frontal positions, looped moraines and degree of crevassing. The remaining three glaciers studied, Besselsbreen, Koristkabreen and its unnamed neighbour, have no clear historical record of surging. The advanced position of Besselsbreen beyond the coast of Barentsøya and its very low surface profile (Fig. 9C) suggest the presence of stagnant ice that would be typical of the quiescent phase of a surge cycle. 1936 photographs of Koristkabreen and the adjacent glacier are less easy to interpret, although both glaciers clearly protrude beyond the outer coast as marine ice lobes (Fig. 11C). Thus, although these three glaciers, and Besselsbreen in particular, may well be of surge-type, there is little historical observational evidence to confirm this. Thus, it is also possible that these three glaciers have retreated from a maximum Little Ice Age position, which was probably achieved sometime in the late 19th Century. However, it should also be remembered that many (e.g. Dowdeswell et al., 1991; Hagen et al., 1993;

Hamilton and Dowdeswell, 1996; Jiskoot et al., 1998), and arguably a majority (Lefauconnier and Hagen, 1991; Sund et al., 2009), of Svalbard glaciers, especially those reaching tidewater, are of surge-type.

Although the Holocene marine sediments offshore of Svalbard are, for the most part, poorly controlled chronologically, it is also possible that glacier surges, some perhaps pre-dating the Little Ice Age of the past few hundred years, may be present in the offshore record. Such evidence is likely to be fragmentary, however, given likely reworking and buried by fast-flowing ice if multiple surges have taken place over a period that may extend as far back as the last regional deglaciation from the Late Weichselian ice-sheet maximum.

7.2 Modern Glaciological Analogues from the Eurasian Arctic

Oblique aerial photographs from 1936 held by the Norsk Polarinstitutt, together with earlier historical maps and sketches, provide an important window on past fluctuations and surges of the nine glaciers we have investigated from Olav V Land and Barentsøya (Fig. 15). In addition, several very recent and ongoing surges of ice-cap drainage basins of eastern Svalbard and in the Russian Arctic archipelago of Severnaya Zemlya provide useful contemporary analogues for ice advance into open-marine settings (e.g. Dowdeswell et al., 2008, 2010; Strozzi et al., 2017). Modern surges in which ice is advancing rapidly beyond the outer coastline of the Austfonna ice cap on Nordaustlandet (McMillan et al., 2014; Dunse et al., 2015) and into open-marine water offshore of Vavilov Ice Cap in Severnaya Zemlya (Willis et al., Submitted) are producing heavily crevassed ice lobes of several kilometres in length (Fig. 16A-B). Sometimes the ice front is observed to break into several filaments or fingers as the surge progresses (Fig. 16C).

It is clear that the generally lobate form and dimensions of these modern, active glacier surges is very similar to that of the submarine basins defined by terminal moraines in our multibeam bathymetric data (Fig. 13). In addition, the observed breakup of the modern glacier terminus into fingers observed during high-velocity contemporary surging (Fig. 16C) may account for the indentations in the ice-proximal flanks of several terminal moraines imaged by multibeam echo-sounder, which are particularly notable at Hannbreen and Koristkabreen (Figs. 10A, 11A). It may also assist in explaining more unusual submarine features such as the finger-like structures extending beyond the main terminal moraine of the unnamed glacier (Kw) in Figure 11A. Similar finger-like geomorphic forms have been reported from the floor of proglacial lake Hvítárvatn beyond the Langjökull ice cap in Iceland (Geirsdóttir et al., 2016).

Sections through recently deposited moraine ridges of 5 to 15 m in height, observed about 30 km north of the contemporary surge advance of Austfonna, also demonstrate that ice thrusting has taken place to build a series of stacked ridge crests (Fig. 16D). Such features may be similar to those observed in multibeam bathymetry of the easternmost part of the Negribreen submarine terminal moraine (Fig. 5A), where multiple sub-parallel crests are mapped (Fig. 5B). Ice thrusting is a known process at surge-type glaciers (Lawson et al., 1994) and similar stacked thrust moraines have also been observed in Late Quaternary glacial sediments (e.g. Hart and Boulton, 1991).

8. Conclusions

The seafloor morphology in front of nine glaciers terminating in open-marine settings in eastern Svalbard has been investigated using multibeam swath-bathymetric data. Most of these tidewater glaciers have either been observed to surge or have looped surface moraines and ice structures indicative of past surge activity. Historical information on the fluctuations of these tidewater glaciers over the past century or so shows that the seafloor to about 5 to 20 km offshore of the present glacier termini has been exposed for less than a century or so. The submarine geomorphology is very well preserved, providing a suite of glacial landforms relating to the last major advance or surge of each marine-terminating glacier drainage basin.

During these ice advances into the open-marine environment, an assemblage of landforms has been produced on the seafloor (Fig. 13) which is imaged at very high resolution by multibeam echo-sounding. Individual landform types are divided into three categories; those formed subglacially, ice marginally and beyond the ice front in a glacier-influenced open-marine setting.

(a) Ice-overridden transverse ridges and streamlined subglacial landforms include curvilinear MSGLs and lineations, blunt-nosed elongate drumlins and medial moraines. Smaller ridges form a complex boxwork or rhombohedral pattern, linked to the squeezing of soft sediment into basal crevasses. Meltwater-related subglacial landforms include eskers and channels.

(b) Ice-marginal landforms, produced close to grounded tidewater glacier termini, include a variety of transverse-to-flow ridges; from large terminal moraines formed at the maximum position of grounded ice advance to small delicate retreat moraines only a few metres high. Outer terminal moraine flanks are typically associated with well-defined debris-flow lobes, whereas the inner flanks sometimes show marked indentations, interpreted to represent the finger-like margins of advancing surge-type glaciers. Further ice-marginal landforms are distinctive flat-floored crater-like kettle holes.

(c) In the marine waters beyond tidewater glacier margins, the keels of drifting icebergs produce irregular to chaotic patterns of ploughmarks. In addition, glacimarine sedimentation by the rain-out of fine-grained debris from meltwater plumes begins to bury seafloor glacial landforms subsequent to their formation and exposure by glacier retreat.

A schematic plan-view landform assemblage model for tidewater glaciers advancing into open-marine settings is illustrated in Figure 14. The broad-scale arcuate geometry of terminal moraines marking the surge outer limit provides a distinctive component of the assemblage, marking the limits of surge or Little Ice Age advance unconstrained by fjord walls. The submarine basin(s) exposed inside these outer moraine ridges when ice retreats during the quiescent phase of the surge cycle contain a further suite of landforms. The assemblage of landforms consists of several individual features, produced subglacially and ice-marginally, the pattern of which is shown in order of timing of deposition and stratigraphic superposition in Figure 14.

This new schematic model of an open-marine surge-type landform assemblage can be compared with earlier models that were based on submarine landforms associated with surges in the more topographically constrained setting of Spitsbergen fjords, differing in several ways: (i) the overall shape of the open-marine assemblage is arcuate, reflecting the lack of constraining fjord walls; (ii) the ice-proximal sides of terminal moraine ridges are often indented, reflecting the sometimes irregular and broken termini of tidewater glaciers surging into open water; (iii) the pattern of streamlined lineations is generally fan-shaped; (iv) crater-like kettle holes are found at the inner lateral margins of many submarine basins, linked to ice stagnation in shallow water; (v) systems of eskers and channels are prominent, associated with indentations in the retreating ice front.

Modern glaciological analogues from the Eurasian Arctic include several ongoing surges of ice-cap drainage basins in eastern Svalbard and Russian Severnaya Zemlya. They provide contemporary observations of ice advance into open-marine settings. Modern surges are producing heavily crevassed ice lobes of several kilometres in length, where the ice front sometimes breaks into several filaments or fingers as the surge progresses. The generally lobate form and dimensions of these modern, active glacier surges is very similar to that of the submarine basins defined by terminal moraines in our multibeam bathymetric data (Figs. 13, 14).

Acknowledgements

We thank the Norwegian Mapping Authority Hydrographic Service for granting access to their multibeam swath-bathymetric datasets from eastern Svalbard and Norsk Polarinstitutt for the use of their vertical and oblique aerial photographs of Svalbard glaciers. Dr A.F. Glazovsky kindly provided the photograph of Vavilov Ice Cap used in Figure 16.

References

Andreassen, K., Winsborrow, M.C.M., Bjarnadóttir, L.R., Rüther, D.C., 2014. Ice stream retreat dynamics inferred from an assemblage of landforms in the northern Barents Sea. Quat. Sci. Rev. 92, 246-257.

Barrie, J.V., Lewis, C.F.M., Parrott, D.R., Collins, W.T., 1992. Submersible observations of an iceberg pit and scour on the Grand Banks of Newfoundland. Geo-Mar. Lett. 12, 1-6.

Bassford, R.P., Siegert, M.J., Dowdeswell, J.A., Oerlemans, J., Glazovsky, A.F., Macheret, Y.Y., 2006. Quantifying the mass balance of ice caps on Severnaya Zemlya, Russian High Arctic. In: Climate and mass balance of the Vavilov Ice Cap. Arct. Antarct. Alp. Res. 38, 1-12.

Batchelor, C.L., Dowdeswell, J.A., Dowdeswell, E.K., Todd, B.J., 2016. A subglacial landform assemblage on the outer shelf of M'Clure Strait, Canadian Arctic, ploughed by iceberg keels. In: Dowdeswell, J.A. et al., (Eds.), Atlas of Submarine Glacial Landforms: Modern, Quaternary and Ancient. Geol. Soc. London, Mem. 46, 337-340.

Benn, D.I., Evans, D.J.A., 2010. Glaciers and Glaciation (2nd Edition). Arnold Publishers, London.

Bjarnadóttir, L.R., Ottesen, D., Dowdeswell, J.A., Bugge, T., 2016. Unusual iceberg ploughmarks on the Norwegian continental shelf. In: Dowdeswell, J.A. et al., (Eds), Atlas of Submarine Glacial Landforms: Modern, Quaternary and Ancient. Geol. Soc. London, Mem. 46, 283-284.

Boulton, G.S., 1986. Push-moraines and glacier-contact fans in marine and terrestrial environments. Sedimentology 33, 677-698.

Boulton, G.S., van der Meer, J.J.M., Hart, J., Beets, D., Ruegg, G.H.J., van der Wateren, F.M., Jarvis, J., 1996. Till and moraine emplacement in a deforming bed surge - An example from a marine environment. Quat. Sci. Rev. 15, 961-987.

Burton, D.J., Dowdeswell, J.A., Hogan, K.A. and Noormets, R., 2016. Marginal fluctuations of a Svalbard surge-type glacier, Blomstrandbreen, since the Little Ice Age: a record of three surges. Arct. Antarct. Alp. Res. 48, 411-426.

Clark, C.D., 1993. Mega-scale glacial lineations and cross-cutting landforms. Earth Surf. Process. Landf. 18, 1-29.

Clark, C.D., 1994. Large-scale ice-moulding: A discussion of genesis and glaciological significance. Sed. Geol. 91, 253-268.

Clark, C.D., Hughes, A.L.C., Greenwood, S.L., Spagnolo, M., Ng, F.S.L., 2009. Size and shape characteristics of drumlins, derived from a large sample, and associated scaling laws. Quat. Sci. Rev., 28, 677-692.

Cowan, E.A., Seramur, K.C., Powell, R.D., Willems, B.A., Gulick, S.P.S., Jaeger, J.M., 2010. Fjords as temporary sediment traps: History of glacial erosion and deposition in Muir Inlet, Glacier Bay National Park, southeastern Alaska. Geol. Soc. Am. Bull. 122, 1067-1080.

Dowdeswell, E.K., Todd, B.J., Dowdeswell, J.A., 2016. Submarine medial moraines and convergent ice flow, Scott Inlet, Baffin Island, Arctic Canada. In: Dowdeswell, J.A. et al., (Eds.), Atlas of Submarine Glacial Landforms: Modern, Quaternary and Ancient. Geol. Soc. London, Mem. 46, 193-194.

Dowdeswell, J.A., 1986. Drainage-basin characteristics of Nordaustlandet ice caps, Svalbard. J. Glaciol. 32, 31-38.

Dowdeswell, J.A., 1989. On the nature of Svalbard icebergs. J. Glaciol. 35, 224-234.

Dowdeswell, J.A., Bamber, J.L., 1995. On the glaciology of Edgeøya and Barentsøya. Pol. Res. 14, 105-122.

Dowdeswell, J.A., Vásquez, M., 2013. Submarine landforms in the fjords of southern Chile: implications for glacimarine processes and sedimentation in a mild glacier-influenced environment. Quat. Sci. Rev. 64, 1-19.

Dowdeswell, J.A., Ottesen, D., 2016a. Submarine landform-assemblage for Svalbard surge-type tidewater glaciers. In: Dowdeswell, J.A. et al., (Eds.), Atlas of Submarine Glacial Landforms: Modern, Quaternary and Ancient. Geol. Soc. London, Mem. 46, 151-154.

Dowdeswell, J.A., Ottesen, D., 2016b. Eskers formed at the beds of modern surge-type tidewater glaciers in Spitsbergen. In: Dowdeswell, J.A. et al., (Eds.), Atlas of Submarine Glacial Landforms: Modern, Quaternary and Ancient. Geol. Soc. London, Mem. 46, 83-84.

Dowdeswell, J.A., Hamilton, G.S., Hagen, J.O., 1991. The duration of the active phase on surge-type glaciers – contrasts between Svalbard and other regions. J. Glaciol. 37, 388-400.

Dowdeswell, J.A., Villinger, H., Whittington, R., Marienfeld, P., 1993. Iceberg scouring in Scoresby Sund and on the East Greenland continental shelf. Mar. Geol. 111, 37-53.

Dowdeswell, J.A., Hodgkins, R., Nuttall, A.M., Hagen, J.O., Hamilton, G.S., 1995. Mass-balance change as a control on the frequency and occurrence of glacier surges in Svalbard, Norwegian High Arctic. Geophys. Res. Lett. 22, 2909-2912.

Dowdeswell, J.A., Elverhøi, A., Spielhagen, R., 1998. Glacimarine sedimentary processes and facies on the Polar North Atlantic margins, Quat. Sci. Rev. 17, 243-272.

Dowdeswell, J.A., Ó Cofaigh, C., Pudsey, C.J., 2004. Thickness and extent of the subglacial till layer beneath an Antarctic paleo-ice stream. Geology 32, 13-16.

Dowdeswell, J.A., Benham, T.J., Strozzi, T., Hagen, J.O., 2008. Iceberg calving flux and mass balance of the Austfonna ice cap on Nordaustlandet, Svalbard. J. Geophys. Res. 113, doi: 10.1029/ 2007JF000905.

Dowdeswell, J.A., Dowdeswell, E.K., Williams, M., Glazovsky, A.F., 2010. The glaciology of the Russian High Arctic from Landsat imagery. U.S. Geol. Surv. Prof. Paper 1386-F, 94-125.

Dowdeswell, J.A., Solheim, A., Ottesen, D., 2016a. Rhombohedral crevasse-fill ridges at the marine margin of a surging Svalbard ice cap. In: Dowdeswell, J.A. et al., (Eds.), Atlas of Submarine Glacial Landforms: Modern, Quaternary and Ancient. Geol. Soc. London, Mem. 46, 73-74.

Dowdeswell, J.A., Canals, M., Jakobsson, M., Todd, B.J., Dowdeswell, E.K., Hogan K.A., 2016b. The variety and distribution of submarine glacial landforms and implications for ice-sheet reconstruction. In: Dowdeswell, J.A. et al., (Eds.), Atlas of Submarine Glacial Landforms: Modern, Quaternary and Ancient. Geol. Soc. London, Mem. 46, 519-552.

Dowdeswell, J.A., Ottesen, D., Rise, L., 2016c. Skjoldryggen terminal moraine on the mid-Norwegian Shelf. In: Dowdeswell, J.A. et al., (Eds.), Atlas of Submarine Glacial Landforms: Modern, Quaternary and Ancient. Geol. Soc. London, Mem. 46, 249-250.

Dowdeswell, J.A., Ottesen, D., Plassen, L., 2016d. Debris-flow lobes on the distal flanks of terminal moraines in Spitsbergen fjords. In: Dowdeswell, J.A. et al., (Eds.), Atlas of Submarine Glacial Landforms: Modern, Quaternary and Ancient. Geol. Soc. London, Mem. 46, 77-78.

Dunlop, P., Clark, C.D., 2006. The morphological characteristics of ribbed moraine. Quat. Sci. Rev. 25, 1668-1691.

Dunse, T., Schellenberger, T., Hagen, J.O., Kääb, A., Schuler, T.V., Reijmer, C.H., 2015. Glacier-surge mechanisms promted by a hydro-thermodynamic feedback to summer melt. The Cryosphere 9, 197-215.

Eilertsen, R.S., Bøe, R., Hermanns, R., Longva, O., Dahlgren, S., 2016. Kettle holes, 'dead ice' topography and eskers on a lake floor in Telemark, southern Norway. In: Dowdeswell, J.A. et al., (Eds.), Atlas of Submarine Glacial Landforms: Modern, Quaternary and Ancient. Geol. Soc. London, Mem. 46, 113-114.

Elverhøi, A., Lønne, Ø., Seland, R., 1983. Glacimarine sedimentation in a modern fjord environment. Spitsbergen, Pol. Res. 1, 23-42.

Evans, D.J.A., Rea, B.R., 2003. Surging glacier landsystem. In: Evans, D.J.A, (Ed.), Glacial Landsystems, 259-288, Arnold, London.

Flink, A., Noormets, R., Kirchner, N., Benn, D. I., Luckman, A., Lovell, H., 2015. The evolution of a submarine landform record following recent and multiple surges of Tunabreen glacier, Svalbard. Quat. Sci. Rev. 108, 37-50.

Flink, A.E., Noormets, R., Fransner, O., Hogan, K.A., O'Regan, M., Jakobsson, M., 2017. Past ice flow in Wahlenbergfjorden and its implications for late Quaternary ice dynamics in northeastern Svalbard. Quat. Sci. Rev. 163, 162-179.

Fowler, A.C., Murray, T., Ng, F.S.L., 2001. Thermally controlled glacier surging. J. Glaciol. 47, 527-538.

Fransner, O., Noormets, R., Flink, A.E., Hogan, K.A., O'Regan, M., Jakobsson, M., 2017. Glacial landforms and their implications for glacier dynamics in Rijpfjorden and Duvefjorden, northern Nordaustlandet, Svalbard. J. Quat. Sci. 32, 437-455.

Geirsdóttir, A., Miller, G.H., Wattrus, N.J., Bjørnsson, H., Thors, K., 2008. Stabilization of glaciers terminating in closed water bodies: Evidence and broader implications. Geophys. Res. Lett. 35, doi:10.1029/2008GL034432.

Graham, A.G.C., Hodgson, D.A., 2016. Terminal moraines in the fjord basins of sub-Antarctic South Georgia. In: Dowdeswell, J.A. et al., (Eds.), Atlas of Submarine Glacial Landforms: Modern, Quaternary and Ancient. Geol. Soc. London, Mem. 46, 67-68.

Greenwood, S.L., Jakobsson, M., Hell, B., Olas, H., 2016. Esker systems in the Gulf of Bothnia. In: Dowdeswell, J.A. et al., (Eds.), Atlas of Submarine Glacial Landforms: Modern, Quaternary and Ancient. Geol. Soc. London, Mem. 46, 209-210.

Grove, J.M., 1988. The Little Ice Age. Methuen, London, 498 pp.

Hagen, J.O., Liestøl, O., Roland, E., Jørgensen, T., 1993. Glacier Atlas of Svalbard and Jan Mayen. Norsk Polarinstitutt, 141 pp.

Hamilton, G.S., Dowdeswell, J.A., 1996. Controls on glacier surging in Svalbard. J. Glaciol. 42, 157-168.

Hart, J.K., Boulton, G.S., 1991. The interrelation of glaciotectonic and glaciodepositional processes within the glacial environment. Quat. Sci. Rev. 10, 335-350.

Heuglin, T.V., 1872. Reisen nach dem Nordpolarmeer on den jahren 1870-71. Map Original karte von

Ost-Spitsbergen zur Ubersicht von Th V Heuglin's Aufnahmen, 1870.

Hughes, A.L.C., Gyllencreutz, R., Lohne, Ø.S., Mangerud, J., Svendsen, J.I., 2016. The last Eurasian ice sheets – a chronological database and time-slice reconstruction, DATED-1. Boreas 45, 1-45.

Jakobsson, M., Gyllencreutz, R., Mayer, L.A., Dowdeswell, J.A., Canals, M., Todd, B.J., Dowdeswell, E.K., Hogan K.A., Larter, R.D., 2016. Mapping submarine glacial landforms using acoustic methods. In: Dowdeswell, J.A. et al., (Eds.), Atlas of Submarine Glacial Landforms: Modern, Quaternary and Ancient. Geol. Soc. London, Mem. 46, 17-40.

Jiskoot, H., Boyle, P., Murray, T., 1998. The incidence of glacier surging in Svalbard: evidence from multivariate statistics. Comp. and Geosci. 24, 387-399.

Jiskoot, H., Murray, T., Boyle, P., 2000. Controls on the distribution of surge-type glaciers in Svalbard. J. Glaciol. 46, 412-422.

Kamb, B., 1987. Glacier surge mechanism based on linked cavity configuration of the basal water conduit system. J. Geophys. Res. 92, 9083-9100.

Kamb, B., Raymond, C.F., Harrison, W.D., Engelhardt, H., Echelmeyer, K.A., Humphrey, N., Brugman, M.M., Pfeffer, T., 1985. Glacier surge mechanism – 1982-1983 surge of Variegated Glacier, Alaska. Science 227, 469-479.

King, E.C., Hindmarsh, R.C.A., Stokes, C.R., 2009. Formation of mega-scale glacial lineations observed beneath a West Antarctic ice stream. Nat. Geosci. 2, 585-58

Lawson, D.E., 1979. Sedimentological analysis of the western terminus region of the Matanuska Glacier, Alaska. Cold Regions Research and Engineering Laboratory Report, 79-9, Hanover, New Hampshire.

Lawson, W.J., Sharp, M., Hambrey, M.J., 1994. The structural geology of a surge-type glacier. J. Struct. Geol. 16, 1447-1462.

Lefauconnier, B., Hagen, J.O., 1991. Surging and calving glaciers in Eastern Svalbard. Norsk Polarinstitutt Medd. 116, 130 pp.

Liestøl, O., 1969. Glacier surges in West Spitsbergen. Can. J. Earth Sci. 6, 895-897.

Lindén, M., Möller, P., 2005. Marginal formation of De Geer moraines and their implications to the dynamics of grounding-line recession. J. Quat. Sci. 20, 113-133.

Lowe, A.L., Anderson, J.B., 2003. Evidence for abundant subglacial meltwater beneath the paleo-ice sheet in Pine Island Bay, Antarctica. J. Glaciol. 49, 125-138.

Lønne, I., Nemec, W., Blikra, L.H., Lauritsen, T., 2001. Sedimentary architecture and dynamics of a marine ice-contact system. J. Sed. Res. 71, 922-943.

McMillan, M., Shepherd, A., Gourmelen, N., Dehecq, A., Leeson, A., Ridout, A., Flament, T., Hogg, A., Gilbert, L., Benham, T., van den Broeke, M., Dowdeswell, J.A., Fettweis, X., Noel, B., Strozzi, T., 2014. Rapid dynamic activation of a marine-based Arctic ice cap. Geophys. Res. Lett. 41, 8902-8909.

Meier, M.F., Post, A., 1969. What are glacier surges. Can. J. Earth Sci. 6, 807-817.

Mugford, R.I., Dowdeswell, J.A., 2011. Modeling glacial meltwater plume dynamics and sedimentation in high-latitude fjords. J. Geophys. Res. 116, doi:10.1029/2010JF001735.

Murray, T., Dowdeswell, J.A., Drewry, D.J., Frearson, I., 1998. Geometric evolution and ice dynamics during a surge of Bakaninbreen, Svalbard. J. Glaciol. 44, 263-272.

Murray, T., Strozzi, T., Luckman, A., Jiskoot, H., Christakos, P., 2003. Is there a single surge mechanism? Contrasts in dynamics between glacier surges in Svalbard and other regions. J. Geophys. Res. 108, doi:10.1029/2002JB001906.

Nordenskiöld, A.E., 1875. Den Svenska Polarexpeditionen, 1872-1873. K. Svenska Vetenskapsakademiets Handlingar 2, 18, 132 p.

Nye, J.F., 1976. Water flow in glaciers, jökulhlaups and veins. J. Glaciol. 17, 181-207.

Ó Cofaigh, C., Pudsey, C.J., Dowdeswell, J.A., Morris, P., 2002. Evolution of subglacial bedforms along a paleo-ice stream, Antarctic Peninsula continental shelf. Geophys. Res. Lett. 29, doi:10.1029/2001GL014488.

Ó Cofaigh, C., Dowdeswell, J.A., Allen, C.S., Hiemstra, J., Pudsey, C.J., Evans, J., Evans, D.J.A., 2005. Flow dynamics and till genesis associated with a marine-based Antarctic palaeo-ice stream. Quat. Sci. Rev. 24, 709-740.

Ottesen, D., Dowdeswell, J.A., 2006. Assemblages of submarine landforms produced by tidewater glaciers in Svalbard. J. Geophys. Res. 111, doi:10.1029/2005JF000330.

Ottesen, D., Dowdeswell, J.A., Benn, D.I., Kristensen, L., Christiansen, H.H., Christensen, O., Hansen, L., Lebesbye, E., Forwick, M., Vorren, T.O., 2008. Submarine landforms characteristic of glacier surges in two Spitsbergen fjords. Quat. Sci. Rev. 27, 1583-1599.

Powell, R.D., 1990. Glacimarine processes at grounding-line fans and their growth to ice-contact deltas. In: Dowdeswell, J.A., Scourse, J.D., (Eds.), Glacimarine Environments: Processes and Sediments, Geol. Soc. London, Spec. Publ. 53, 53-73.

Powell, R.D., Molnia, B.F., 1989. Glacimarine sedimentary processes, facies and morphology of the south-southeast Alaska shelf and fjords. Mar. Geol. 85, 359-390.

Rabot, C., 1900. Les variations de longer des glaciers dans le regions arctiques et boreales. Extrait des Archives des sciences physiques et naturelles, Anees 1899 et 1900. Georg & Co. Editeurs, Geneve et Bale.

Raymond, C.F., 1987. How do glaciers surge – a review. J. Geophys. Res. 92, 9121-9134.

Robinson, P., Dowdeswell, J.A., 2011. Submarine landforms and the behavior of a surging ice cap since the Last Glacial Maximum: the open-marine setting of eastern Austfonna, Svalbard. Mar. Geol. 286, 82-94.

Röthlisberger, H., 1972. Water pressure in intra- and subglacial channels. J. Glaciol. 11, 177-203.

Rowan, D.E., Péwé, T.L., Péwé, R.H., Stuckenrath, R., 1982. Holocene glacial geology of the Svea Lowland, Spitsbergen, Svalbard. Geografiska Annaler 64A, 35-51.

Schytt, V., 1969. Some comments on glacier surges in eastern Svalbard. Can. J. Earth Sci. 6, 867-871.

Sevestre, H., Benn, D.I., 2015. Climatic and geometric controls on the global distribution of surge-type glaciers: implications for a unified model of surging. J. Glaciol. 61, 646-662.

Sharp, M., 1985a. Sedimentation and stratigraphy at Eyjabakkajökull - an Icelandic surging glacier. Quat. Res. 24, 268-284.

Sharp, M., 1985b. 'Crevasse-fill' ridges – a landform type characteristic of surging glaciers? Geografiska

Annaler 67A, 213-220.

Shreve, R.L., 1972. Movement of water in glaciers. J. Glaciol. 11, 205-214.

Solheim, A., 1985. Submarine evidence of glacier surges. Pol. Res. 4, 91-95.

Solheim, A., 1991. The depositional environment of surging sub-polar tidewater glaciers: a case study of the morphology, sedimentation and sediment properties in a surge affected marine basin outside Nordaustlandet, the Northern Barents Sea. Nor. Polarinst. Skrifter 194, 97 pp.

Solheim, A., Pfirman, S.L., 1985. Sea-floor morphology outside a grounded, surging glacier – Bråsvellbreen, Svalbard. Mar. Geol. 65, 127-143.

Spagnolo, M., Clark, C.D., Ely, J.C., Stokes, C.R., Anderson, J.B., Andreassen, K., Graham, A.G.C., King, E.C., 2014. Size, shape and spatial arrangement of mega-scale glacial lineations from a large and diverse dataset. Earth Surf. Process. Landf. 39, 1432-1448.

Sund, M., Eiken, T., Hagen, J.O., Kaab, A., 2009. Svalbard surge dynamics derived from geometric changes. Ann. Glaciol. 50, 50-60.

Sund, M., Lauknes, T.R., Eiken, T., 2014. Surge dynamics in the Nathorstbreen glacier system, Svalbard. The Cryosphere 8, 623-638.

Streuff, K., Forwick, M., Szcucinski, W., Andreassen, K., O Cofaigh, C., 2015. Submarine landform assemblages and sedimentary processes related to glacier surging in Kongsfjorden, Svalbard. Arktos 1, 1-19.

Strozzi, T., Kääb, A., Schellenberger, T., 2017. Frontal destabilization of Stonebreen, Edgeøya, Svalbard. The Cryosphere 11, 553-566.

Svendsen, J.I., Alexanderson, H. Astakhov, V.I., Demidov, I., Dowdeswell, J.A., Funder, S., Gataullin, V., Henriksen, M., Hjort, C., Houmark-Nielsen. M., Hubberten, H.W., Ingolfsson, O., Jakobsson, M., Kjaer, K.H., Larsen, E., Lokrantz, H., Lunkka, J.P., Lyså, A., Mangerud, J., Matiouchkov, A., Murray, A., Møller, P., Niessen, F., Nikolskaya, O., Polyak, L., Saarnisto, M., Siegert, C., Siegert, M.J., Spielhagen, R.F., Stein, R., 2004. Late Quaternary ice-sheet history of northern Eurasia. Quat. Sci. Rev. 23, 1229–1271.

Todd, B.J., 2016. De Geer moraines on German Bank, southern Scotia Shelf of Atlantic Canada. In: Dowdeswell, J.A. et al., (Eds.), Atlas of Submarine Glacial Landforms: Modern, Quaternary and Ancient. Geol. Soc. London, Mem. 46, 259-260.

Todd, B.J., Valentine, P.C., Longva, O., Shaw, J., 2007. Glacial landforms on German Bank, Scotian Shelf: evidence for Late Wisconsinan ice-sheet dynamics and implications for the formation of De Geer moraines. Boreas 36, 148–169.

Vieli, A., Jania, J., Kolondra, L., 2002. The retreat of a tidewater glacier: observations and model calculations on Hansbreen, Spitsbergen. J. Glaciol. 48, 592-600.

Wellner, J.S., Lowe, A.L., Shipp, S.S., Anderson, J.B., 2001. Distribution of glacial geomorphic features on the Antarctic continental shelf and correlation with substrate: implications for ice behaviour. J. Glaciol. 47, 397-411.

Werner, A., 1993. Holocene moraine chronology, Spitsbergen, Svalbard: lichenometric evidence for multiple Neoglacial advances in the Arctic. The Holocene 3, 128-137.

Woodworth-Lynas, C.M.T., Josenhans, H.W., Barrie, J.V., Lewis, C.F.M., Parrott, D.R., 1991. The physical processes of seabed disturbance during iceberg grounding and scouring. Cont. Shelf Res. 11, 939-951.

Figure Captions

Fig. 1. Overview map of the study area in eastern Svalbard with multibeam bathymetric coverage (© Kartverket) in colours. The locations of the major drainage basins and of the study area within Svalbard are inset. Glacial drainage basins shown as dark red lines. Black rectangles locate subsequent figures. Ak is Akademikerbreen, Gi is Ginevrabotnen, Hann is Hannbreen, Hb is Helge Backlundbreen, He is Heleysundet, Koristka is Koristkabreen, Kw is unnamed glacier west of Koristkabreen, Op is Opalbreen, Or is Ordonannsbreen and Pe is Pedasjenkobreen.

Fig. 2. Examples of subglacially produced seafloor features in the study area (© Kartverket). A) MSGLs, Negribreen (located in Fig. 5A). B) Drumlins, Negribreen (Fig. 5A). C) Medial moraine, Negribreen (Fig. 5A). D) Boxwork or rhombohedral crevasse-fill ridges, Besselsbreen (Fig. 9A). E) Esker, Sonklarbreen (Fig. 7A). F) Meltwater channels, Negribreen (Fig. 5A).

Fig. 3. Examples of ice-marginal landforms exposed at the seafloor in the study area (© Kartverket). A) Large moraine ridges (white arrows), Sonklarbreen (located in Fig. 7A). B) Small transverse retreat moraines, Besselsbreen (Fig. 9A). C) Indentations in ice-proximal moraine flank (white arrows), Hannbreen (Fig. 10A). D) Overidden large moraines ridges (one marked as a white dotted line), Negribreen (Fig. 5A). E) Glacigenic debris-flow lobes on ice-distal moraine flank, Koristkabreen (Fig. 11A). F) Kettle holes, partly infilled with sediment, Sonklarbreen (Fig. 7A).

Fig. 4. Glacimarine and related seafloor features in the study area (© Kartverket). A) Iceberg ploughmarks beyond the outmost moraine ridges, east of Olav V Land (located in Fig. 1). B) Basin-fill sediments partially burying moraine ridges (two marked with white arrows), offshore of Hannbreen (Fig. 10A). IPM is iceberg ploughmark. C) Current ripples (white arrow) and D) Sediment drift (white arrow) with sharp advancing front burying glacial features, west of Heleysundet (Fig. 1).

Fig. 5. Negribreen. A) Multibeam bathymetry and 2011 vertical aerial photograph of the modern glacier front (© Kartverket). P is Petermannbreen, K is Kvalrossøya. (1) and (2) mark large moraine ridges. The key for landform interpretation diagrams in this and subsequent figures is inset. B) Interpreted distribution of submarine landforms offshore of Negribreen. C) Oblique aerial photograph of Negribreen and Petermannbreen from 1936 (© Norsk Polarinstitutt). Note medial moraine between Negribreen and Petermannbreen (white arrows). D) Seafloor morphology showing the influence of Kvalrossøya on submarine landforms and past glacier flow. Small coloured circles mark similar positions on Fig. 5D and 5E. E) Oblique aerial photograph of the surface of Negribreen as it flowed over Kvalrossøya during the 1936 surge (© Norsk Polarinstitutt).

Fig. 6. Helge Backlundbreen. A) Multibeam bathymetry and 2011 vertical aerial photograph of the modern glacier front (© Kartverket). lm is lateral moraine, k is kettle hole. White stippled line marks 1936 ice front position. Small coloured circles mark similar positions on Fig. 6A and 6C. B) Interpreted distribution of submarine landforms offshore of Helge Backlundbreen (see key in Fig. 5A). C) Oblique aerial photograph from 1936 (© Norsk Polarinstitutt).

Fig. 7. Sonklarbreen. A) Multibeam bathymetry and 2011 vertical aerial photograph of the modern glacier front (© Kartverket). Black stippled line shows ice front position from 1936 (from Lefauconnier and Hagen, 1991). La is Lamontøya; lm is a lateral moraine ridge also marked in Fig. 7C. B) Interpreted distribution of submarine landforms offshore of Sonklarbreen (see key in Fig. 5A). C) Oblique aerial photograph from 1936 of Sonklarbreen and Helge Backlundbreen (© Norsk Polarinstitutt). Ga is Ganskijbreen; Pe is Pedasjenkobreen.

Fig. 8. Pedasjenkobreen. A) Multibeam bathymetry and 2011 vertical aerial photograph of the modern glacier front (© Kartverket). Black stippled line shows ice front position from 1936 (digitized from Lefauconnier and Hagen, 1991). lm mark lateral moraine ridges also marked in Fig. 8C. B) Interpreted distribution of submarine landforms offshore of Pedasjenkobreen (see key in Fig. 5A). C) Oblique aerial photograph from 1936 (© Norsk Polarinstitutt).

Fig. 9. Besselsbreen. A) Multibeam bathymetry and 2011 vertical aerial photograph of the modern glacier front (© Kartverket). White stippled line locates ice front position from 1936 (digitized from Lefauconnier and Hagen, 1991). B) Interpreted distribution of submarine landforms offshore of Besselsbreen (see key in Fig. 5A). C) Oblique aerial photograph from 1936 (© Norsk Polarinstitutt).

Fig. 10. Hannbreen. A) Multibeam bathymetry and 2011 vertical aerial photograph of the modern glacier front (© Kartverket). Stippled line locates ice front position from 1936 (from Lefauconnier and Hagen, 1991). lm are lateral moraine ridges. B) Interpreted

distribution of submarine landforms offshore of Hannbreen (see key in Fig. 5A). C) Oblique aerial photograph from 1936 (view to the north) (© Norsk Polarinstitutt).

Fig. 11. Koristkabreen and unnamed glacier west of Koristkabreen (Kw). A) Multibeam bathymetry (© Kartverket) and 2011 vertical aerial photograph of the modern glacier fronts (© Norsk Polarinstitutt). Black stippled lines locate ice from positions from 1936 (digitized from Lefauconnier and Hagen, 1991). B) Interpreted distribution of submarine landforms offshore of Koristkabreen and the adjacent unnamed glacier (see key in Fig. 5A). C) Oblique aerial photograph from 1936.

Fig. 12. Hochstetterbreen. A) Multibeam bathymetry and 2011 vertical aerial photograph of the modern glacier front (© Kartverket). Stippled line locates ice front position from 1936 (after Lafauconnier and Hagen, 1991). B) Interpreted distribution of submarine landforms offshore of Hochstetterbreen (see key in Fig. 5A). C) Oblique aerial photograph from 1936 (© Norsk Polarinstitutt).

Fig. 13. Geomorphic map of the distribution of submarine landforms in front of the surging glaciers of eastern Spitsbergen. Gi – Ginevrabotnen, Hb – Helge Backlundbreen, Kw – unnamed glacier west of Koristkabreen, Pe – Pedasjenkobreen.

Fig. 14. Schematic model of submarine landforms linked to glacier surges into the open marine setting of eastern Spitsbergen. Note that, beyond the maximum surge limit, the sea floor is relatively smooth, reflecting rain-out of fine-grained glacimarine debris, but is disturbed by the ploughing action of drifting icebergs.

Fig. 15. Reconstruction of terminus fluctuations on nine eastern Svalbard glaciers since 1860, based on satellite and aerial photographic data and historical maps and sketches (data

mainly from Lefauconnier and Hagen, 1991). Crosses represent observation of ice-front position relative to 2011 ice margins with the points earlier than 1936 have a relatively greater uncertainty in age. The likely timing of surges is marked ‘S’ where a surge has been observed, ‘S?’ when it has been inferred from historical accounts and surface form, and ‘S??’ when there is no specific observational evidence that a surge has taken place. The maximum terminus positions defined from large moraine ridges identified on multibeam imagery are also shown as green dotted line.

Fig. 16. Modern glaciological analogues for Arctic glaciers advancing into open-marine settings. A) Sentinel 2 image (23 July 2016) of ice advance during surges of Basins 2 and 3 of the 8,000 km^2 Austfonna ice cap, Nordaustlandet, eastern Svalbard (Dowdeswell, 1986; Dowdeswell et al., 2008). B) Landsat image of ice advance during a surge of a basin in the 1,770 km^2 Vavilov Ice Cap on October Revolution Island, Severnaya Zemlya, Russian High Arctic (Bassford et al., 2006; Dowdeswell et al., 2010). White arrow indicates the viewing angle of the photograph in panel C. C) May 2016 photograph of the ice front of the surging Vavilov Ice Cap (photo: A.F. Glazovsky). D) Recent photograph of glacitectonic ridges and thrusts in ice, eastern Austfonna, Svalbard (photo: J.A. Dowdeswell). The image is approximately 100 m across.

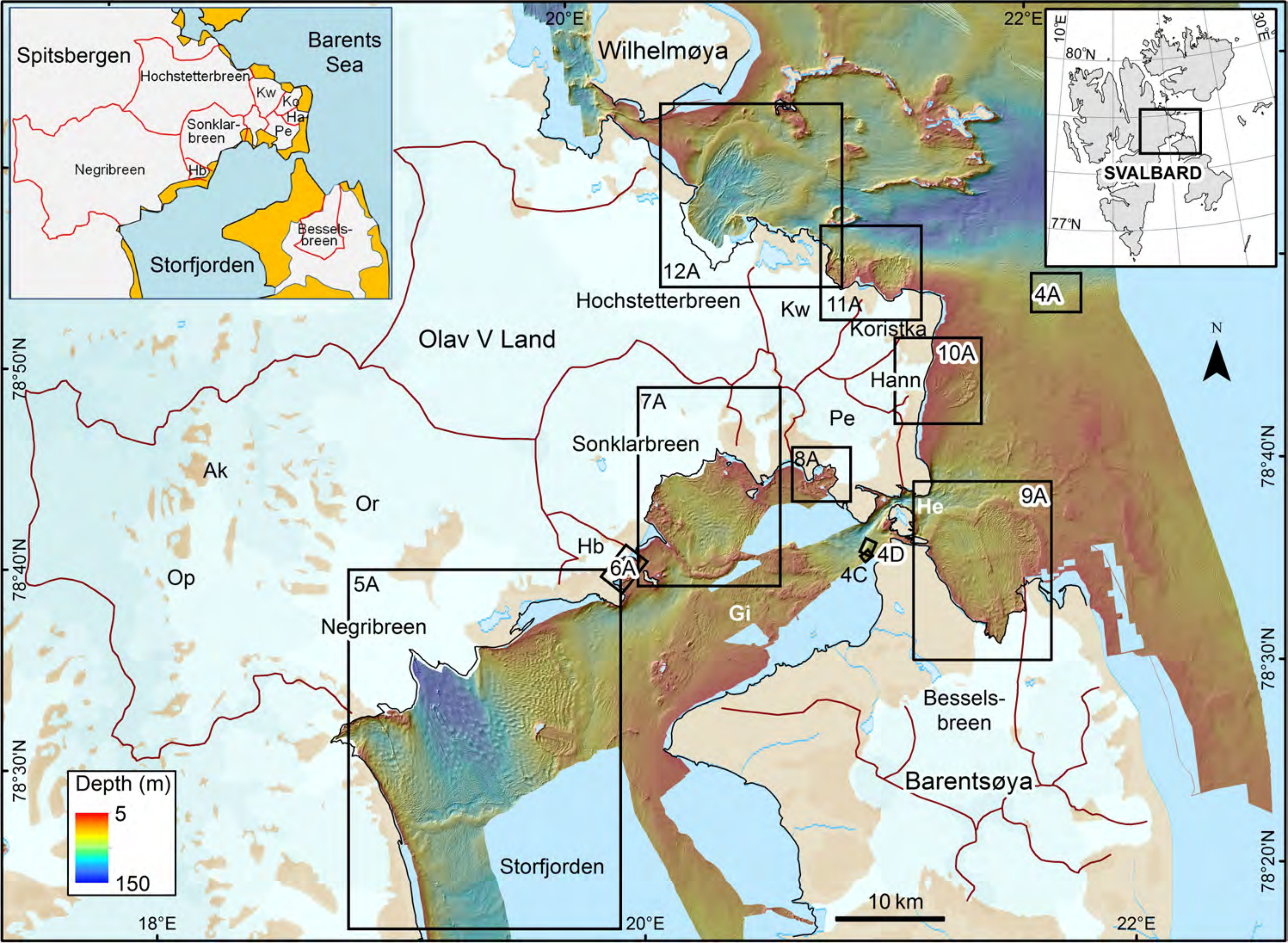

Spitsbergen
Barents Sea
Hochstetterbreen
Kw
Ko
Ha
Sonklar-breen
Pe
Negribreen
Hb
Storfjorden
Bessels-breen
SVALBARD
10°E
30°E
80°N
77°N
20°E
22°E
Wilhelmøya
12A
11A
4A
10A
7A
8A
9A
6A
5A
4C
4D
Hochstetterbreen
Kw
Koristka
Olav V Land
Hann
Pe
Sonklarbreen
Ak
Or
Op
Hb
He
Gi
Negribreen
Bessels-breen
Barentsøya
Storfjorden
Depth (m)
5
150
10 km
N
78°50'N
78°40'N
78°30'N
78°20'N
18°E
20°E
22°E

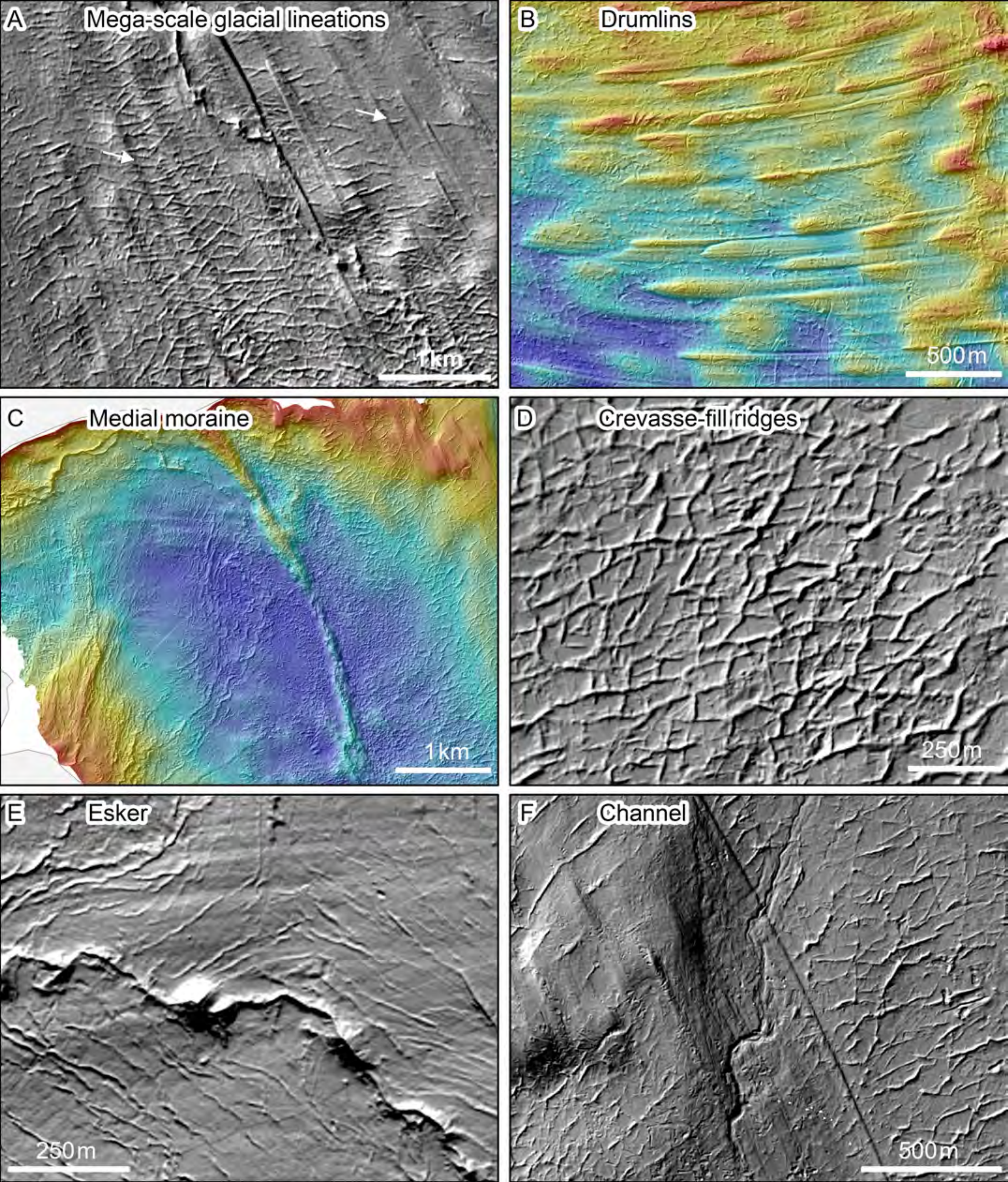
A
Mega-scale glacial lineations
1km
B
Drumlins
500 m
C
Medial moraine
1 km
D
Crevasse-fill ridges
250 m
E
Esker
250 m
F
Channel
500 m

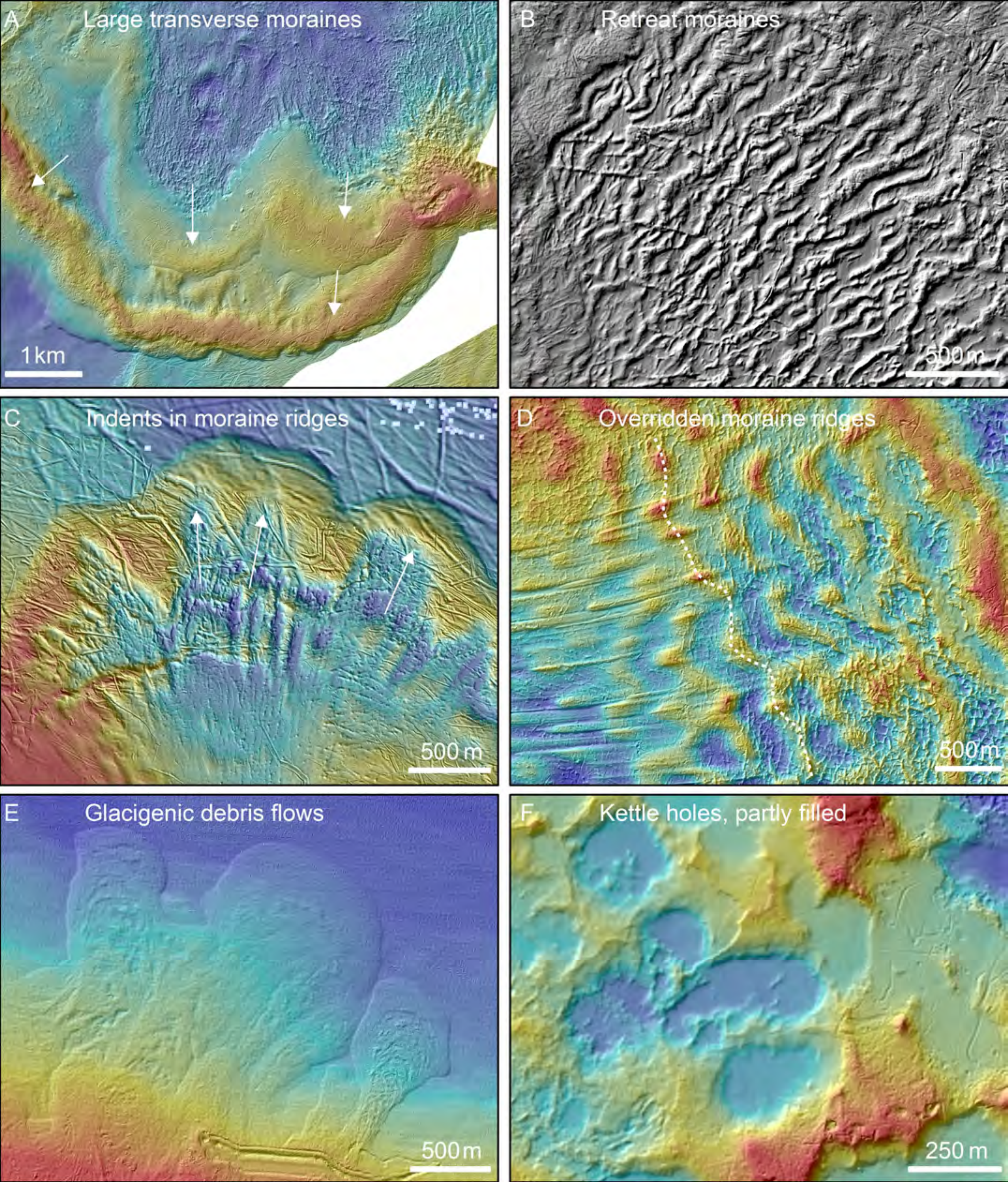
A
Large transverse moraines
1 km
B
Retreat moraines
500 m
C
Indents in moraine ridges
500 m
D
Overridden moraine ridges
500 m
E
Glacigenic debris flows
500 m
F
Kettle holes, partly filled
250 m

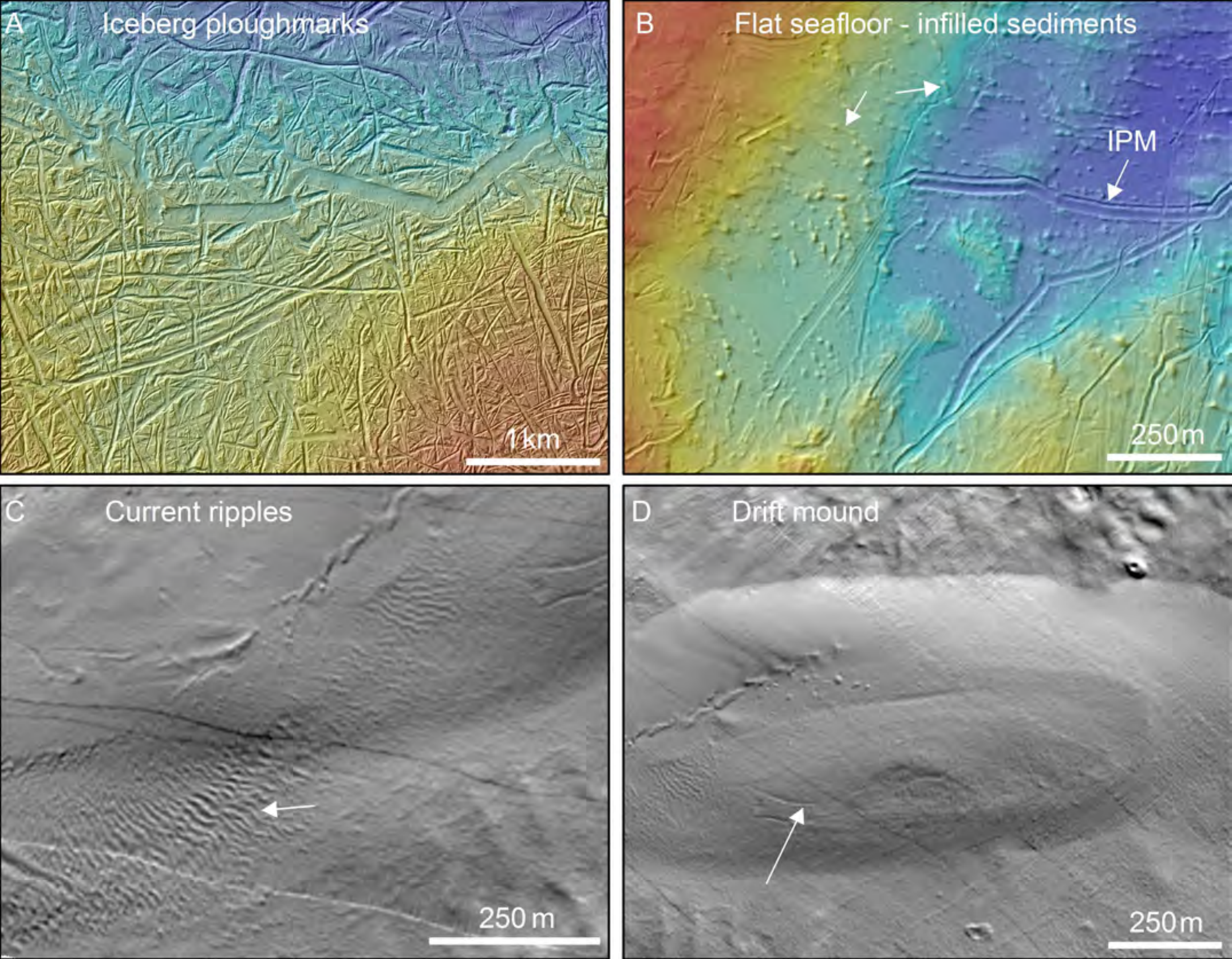
A
Iceberg ploughmarks
1 km
B
Flat seafloor - infilled sediments
IPM
250 m
C
Current ripples
250 m
D
Drift mound
250 m

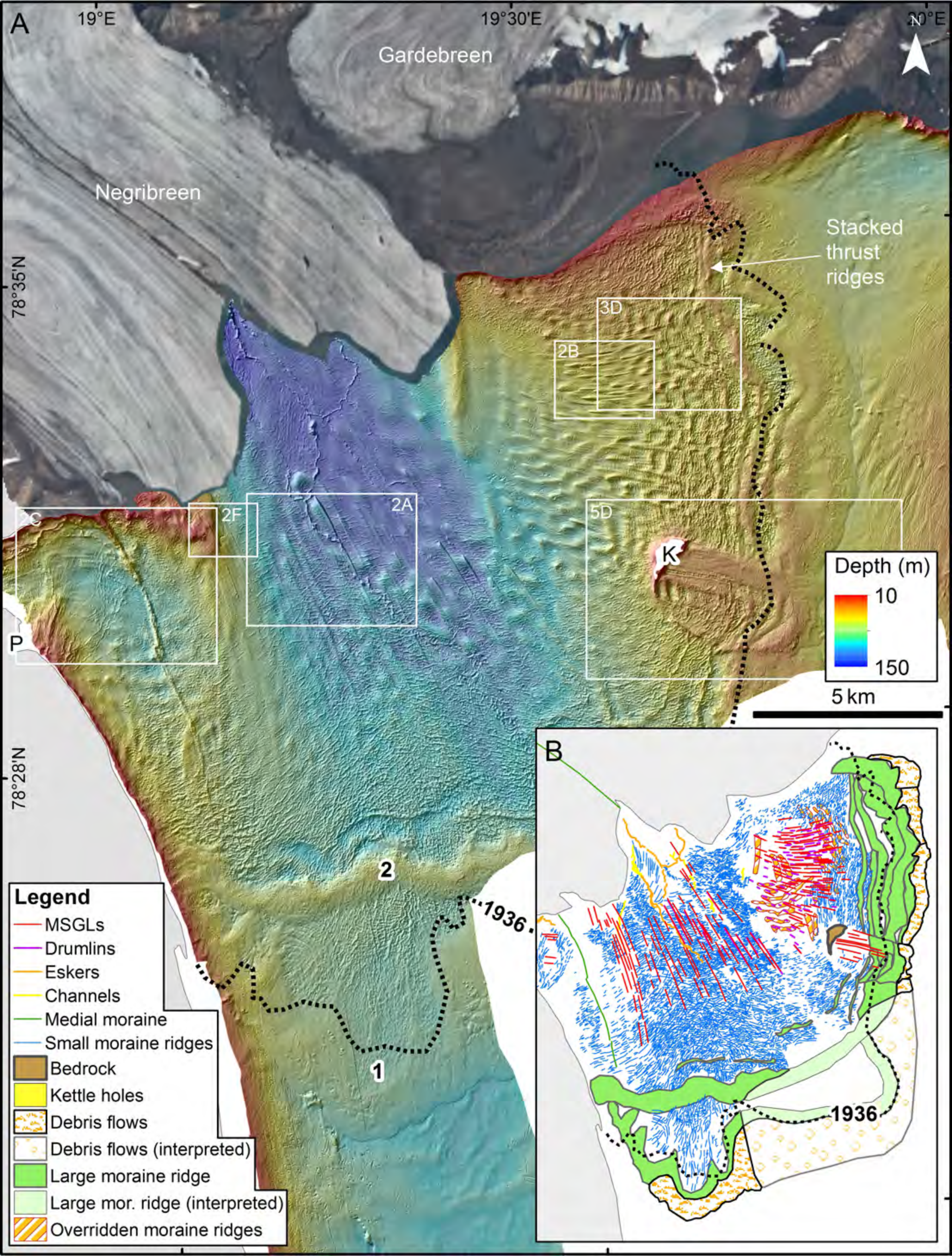

A
19°E
19°30'E
20°E
N
Gardebreen
Negribreen
Stacked
thrust
ridges
78°35'N
3D
2B
2A
2C
2F
5D
K
P
Depth (m)
10
150
5 km
78°28'N
B
2
1
1936
1936
Legend
MSGLs
Drumlins
Eskers
Channels
Medial moraine
Small moraine ridges
Bedrock
Kettle holes
Debris flows
Debris flows (interpreted)
Large moraine ridge
Large mor. ridge (interpreted)
Overridden moraine ridges

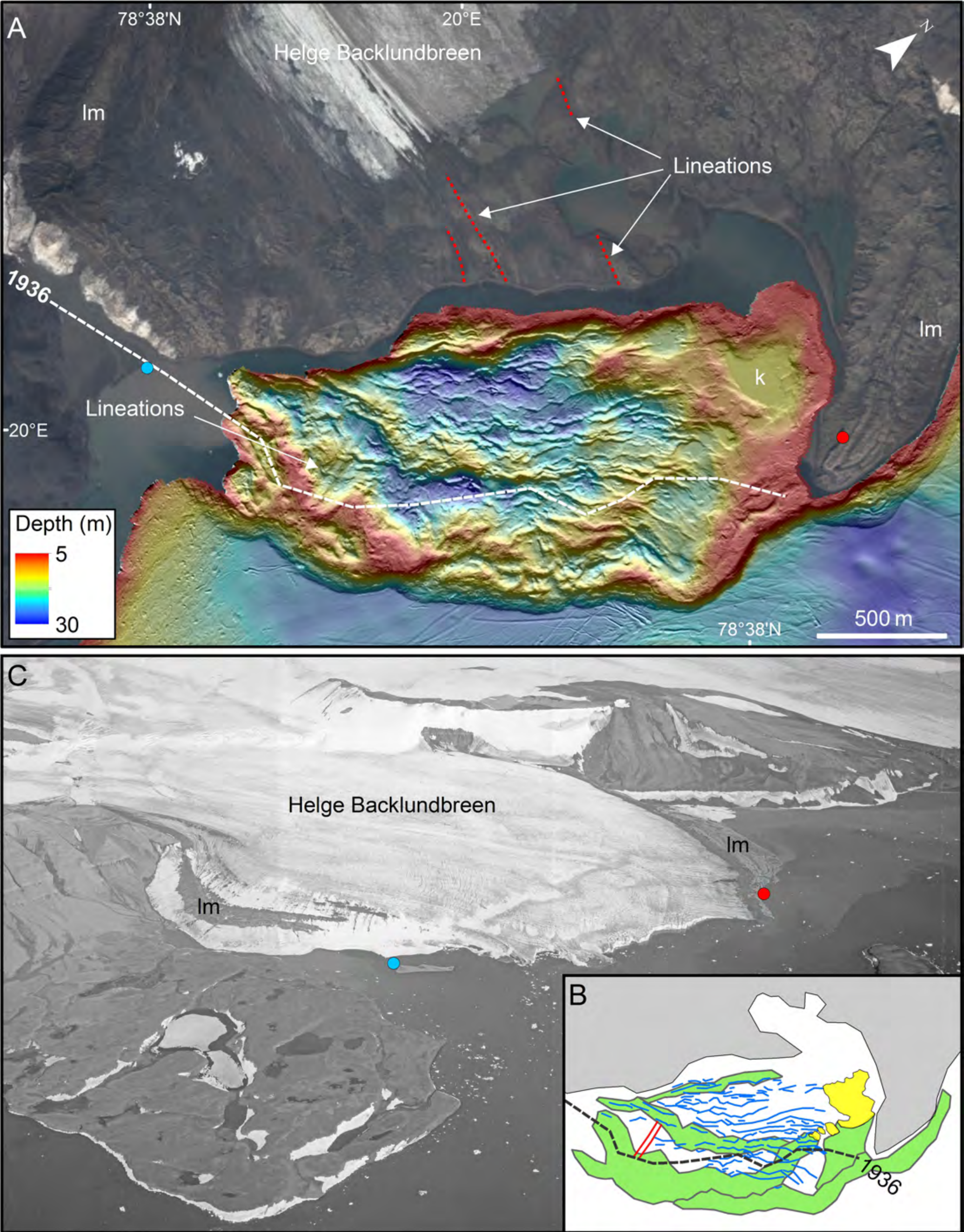

A
78°38'N
20°E
Helge Backlundbreen
lm
Lineations
1936
Lineations
-20°E
k
lm
Depth (m)
5
30
78°38'N
500 m
C
Helge Backlundbreen
lm
lm
B
1936

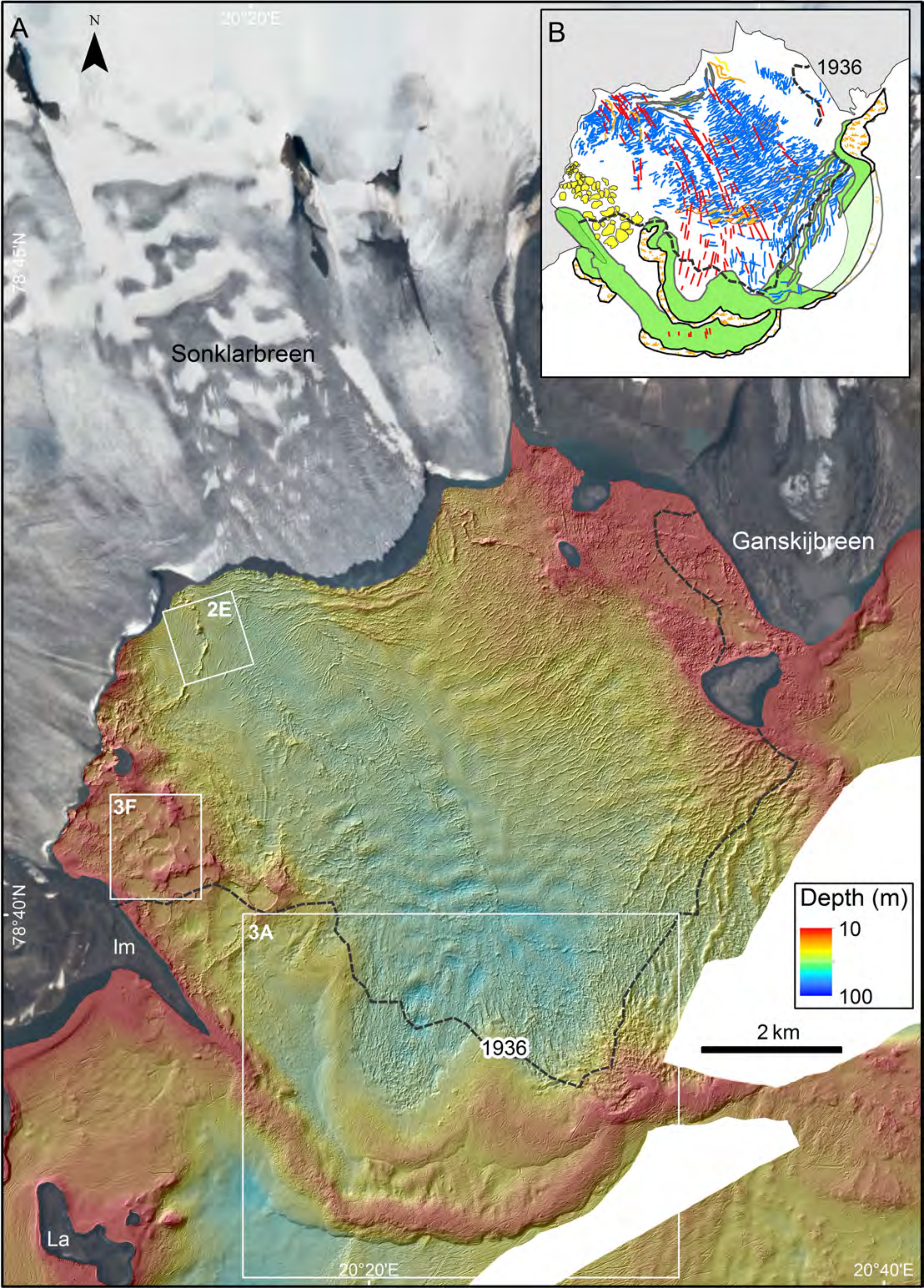
A
N
20°20'E
B
1936
78°45'N
Sonklarbreen
Ganskijbreen
2E
3F
78°40'N
Im
3A
1936
Depth (m)
10
100
2 km
La
20°20'E
20°40'E

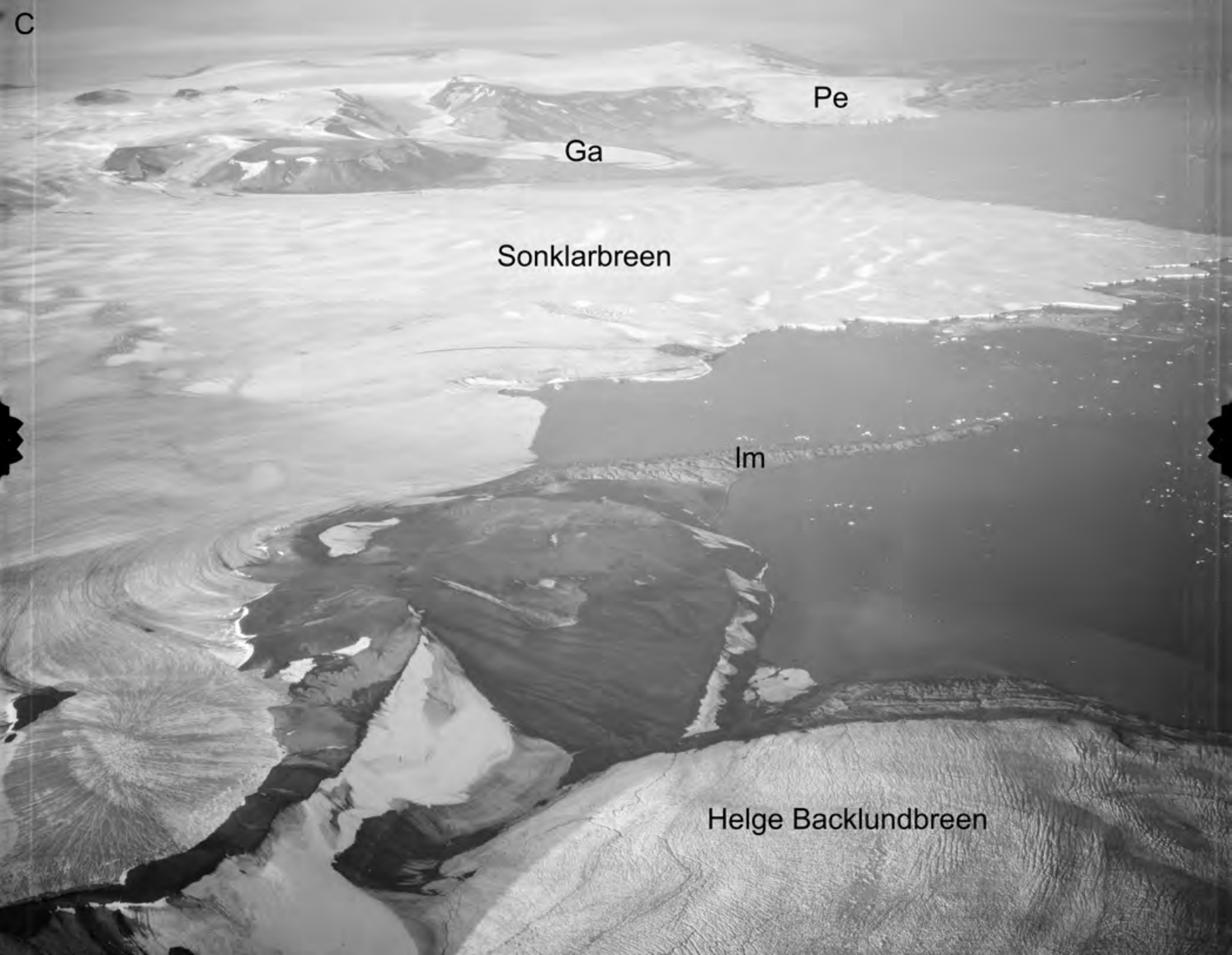
C
Pe
Ga
Sonklarbreen
Im
Helge Backlundbreen

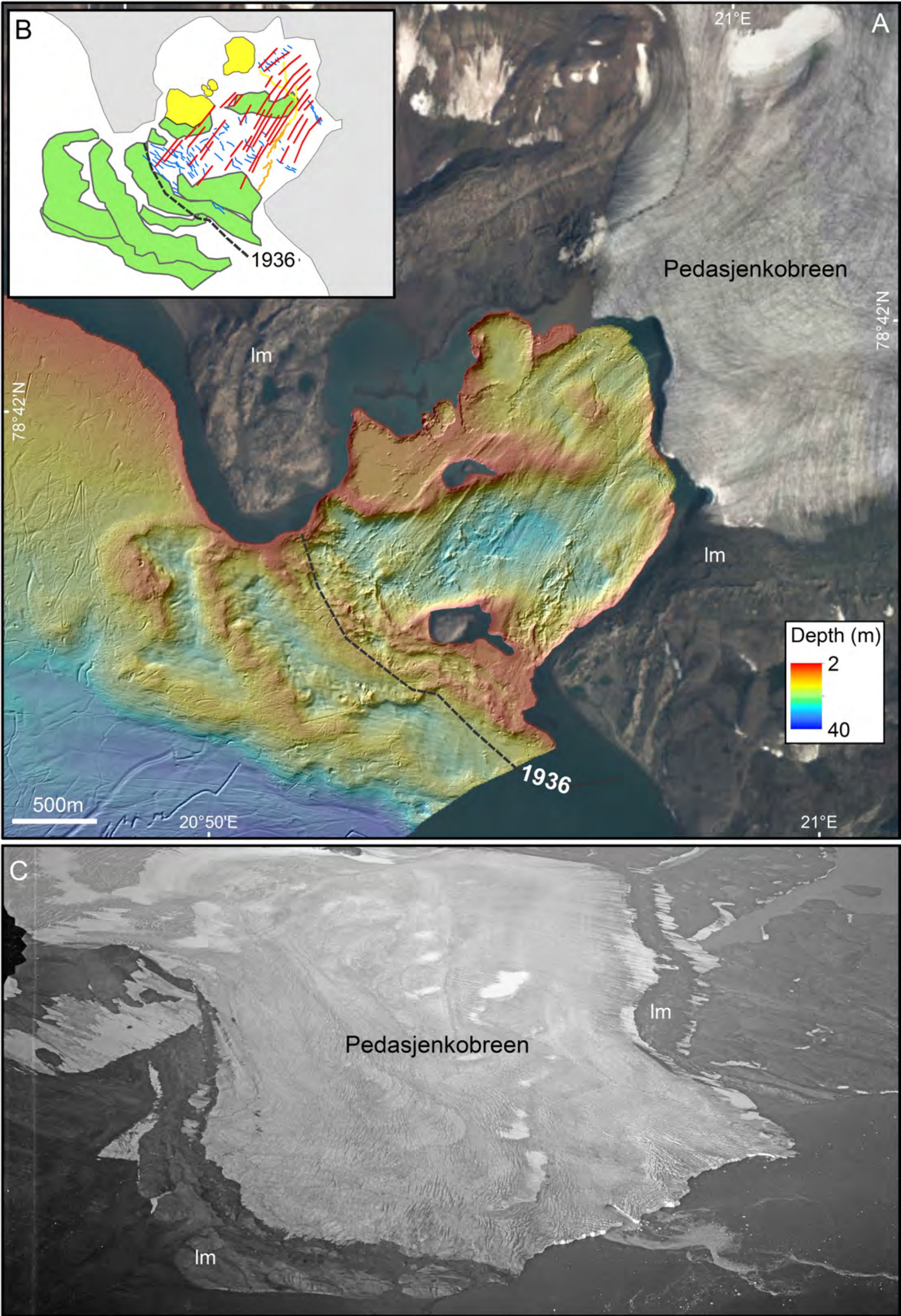

B
1936
21°E
A
Pedasjenkobreen
78°42'N
Im
Im
Depth (m)
2
40
1936
500m
20°50'E
21°E
C
Im
Pedasjenkobreen
Im

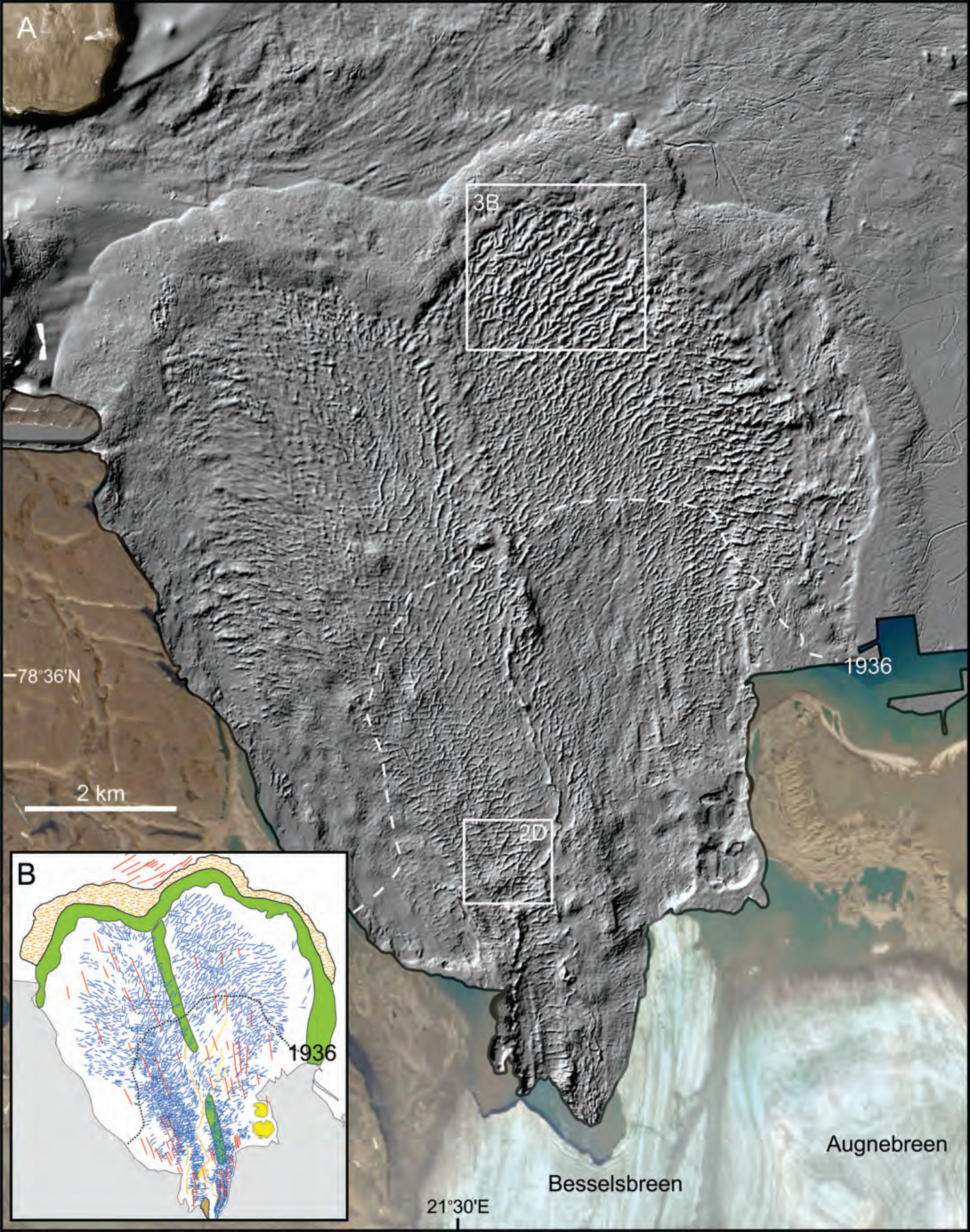
A
3B
1936
78°36'N
2 km
2D
B
1936
Augnebreen
Besselsbreen
21°30'E


C
Augnebreen
Besselsbreen

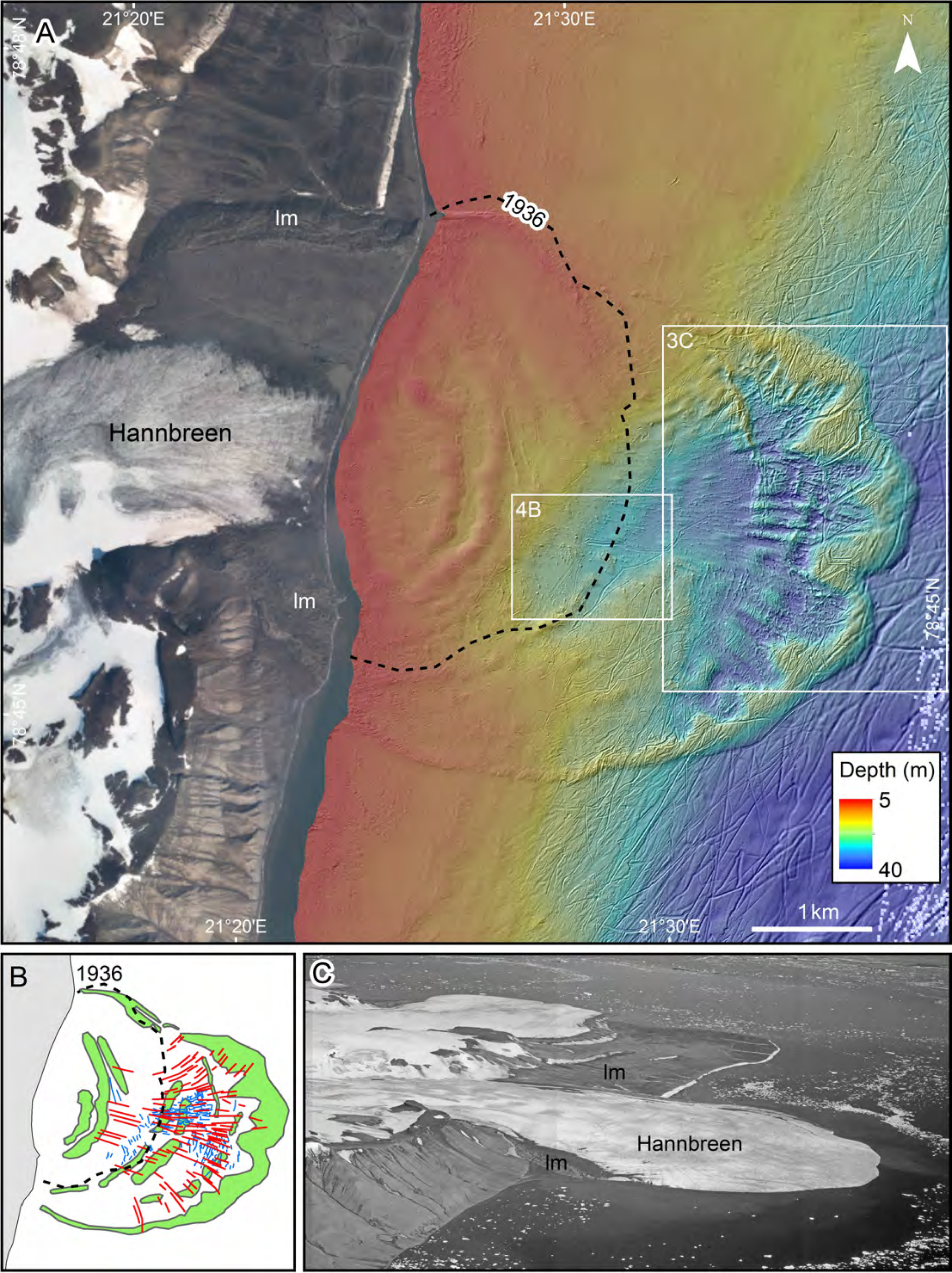
A
21°20'E
21°30'E
78°48'N
N
Im
1936
3C
Hannbreen
4B
Im
78°45'N
78°45'N
Depth (m)
5
40
1 km
21°20'E
21°30'E
B
1936
C
Im
Hannbreen
Im

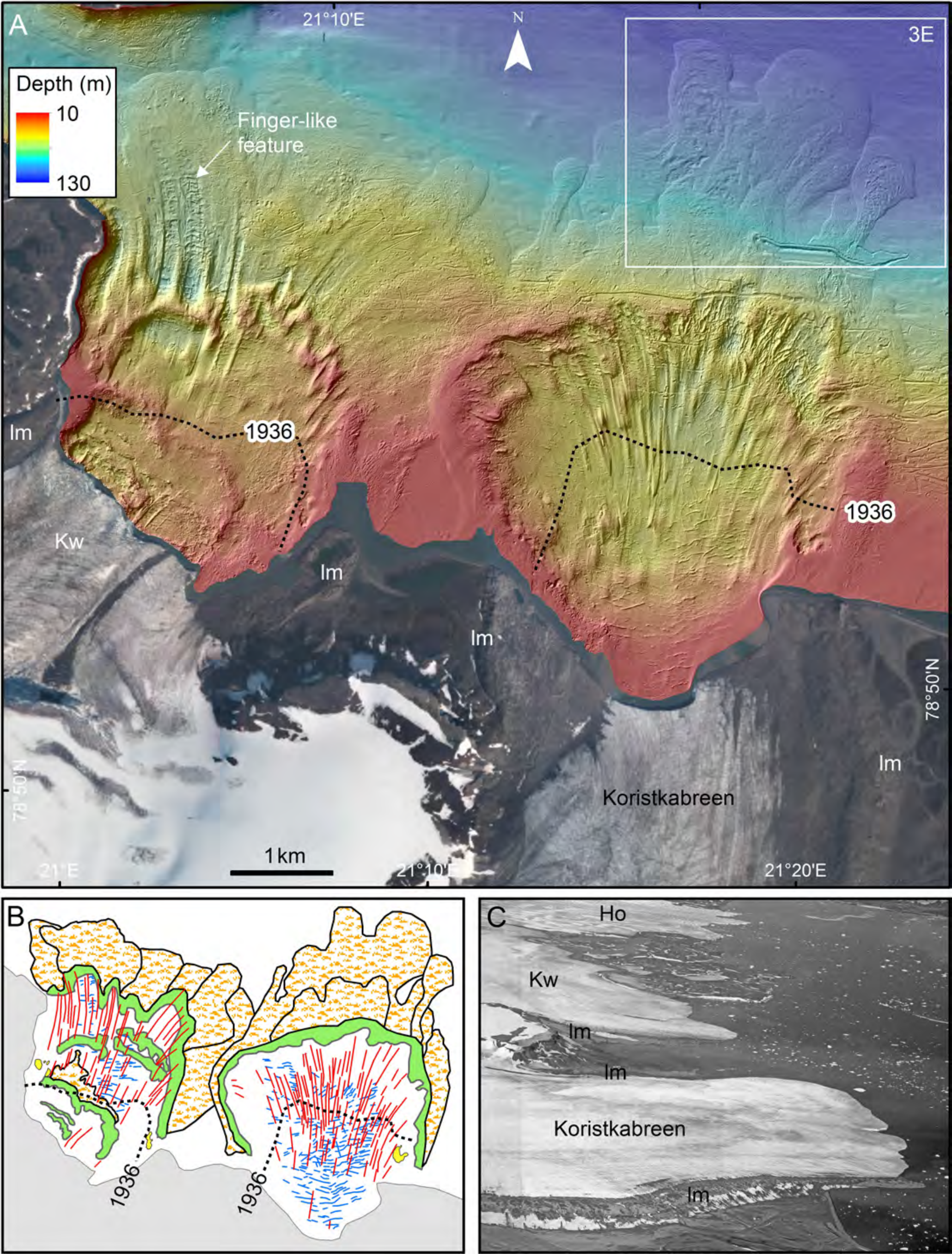

A
21°10'E
N
3E
Depth (m)
10
130
Finger-like feature
Im
1936
1936
Kw
Im
Im
78°50'N
78°50'N
Im
Koristkabreen
1 km
21°E
21°10'E
21°20'E
B
1936
1936
C
Ho
Kw
Im
Im
Koristkabreen
Im

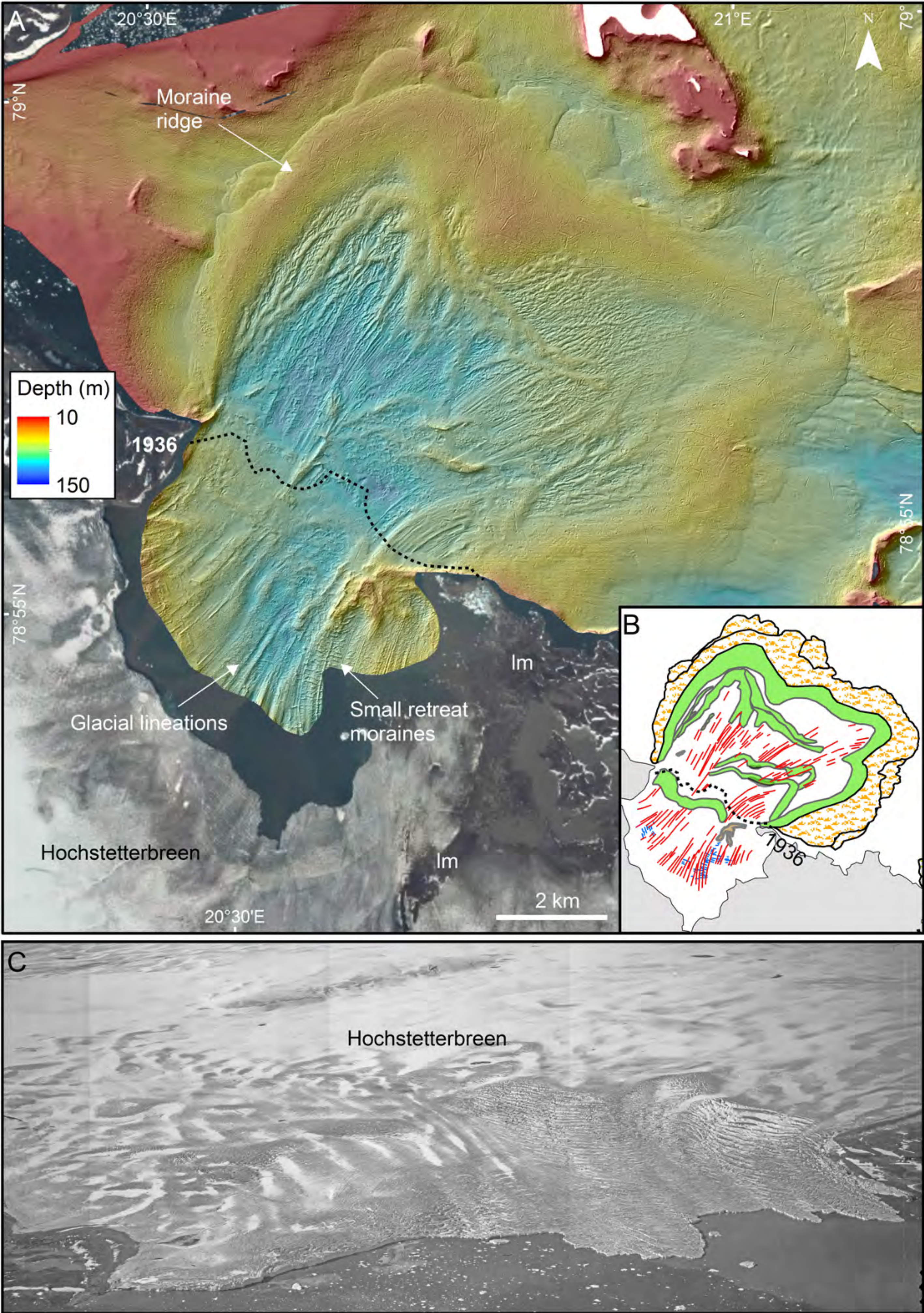
A
20°30'E
21°E
N
79°
79°N
Moraine ridge
Depth (m)
10
150
1936
78°55'N
78°55'N
Glacial lineations
Small retreat moraines
Im
Im
Hochstetterbreen
2 km
20°30'E
B
1936
C
Hochstetterbreen

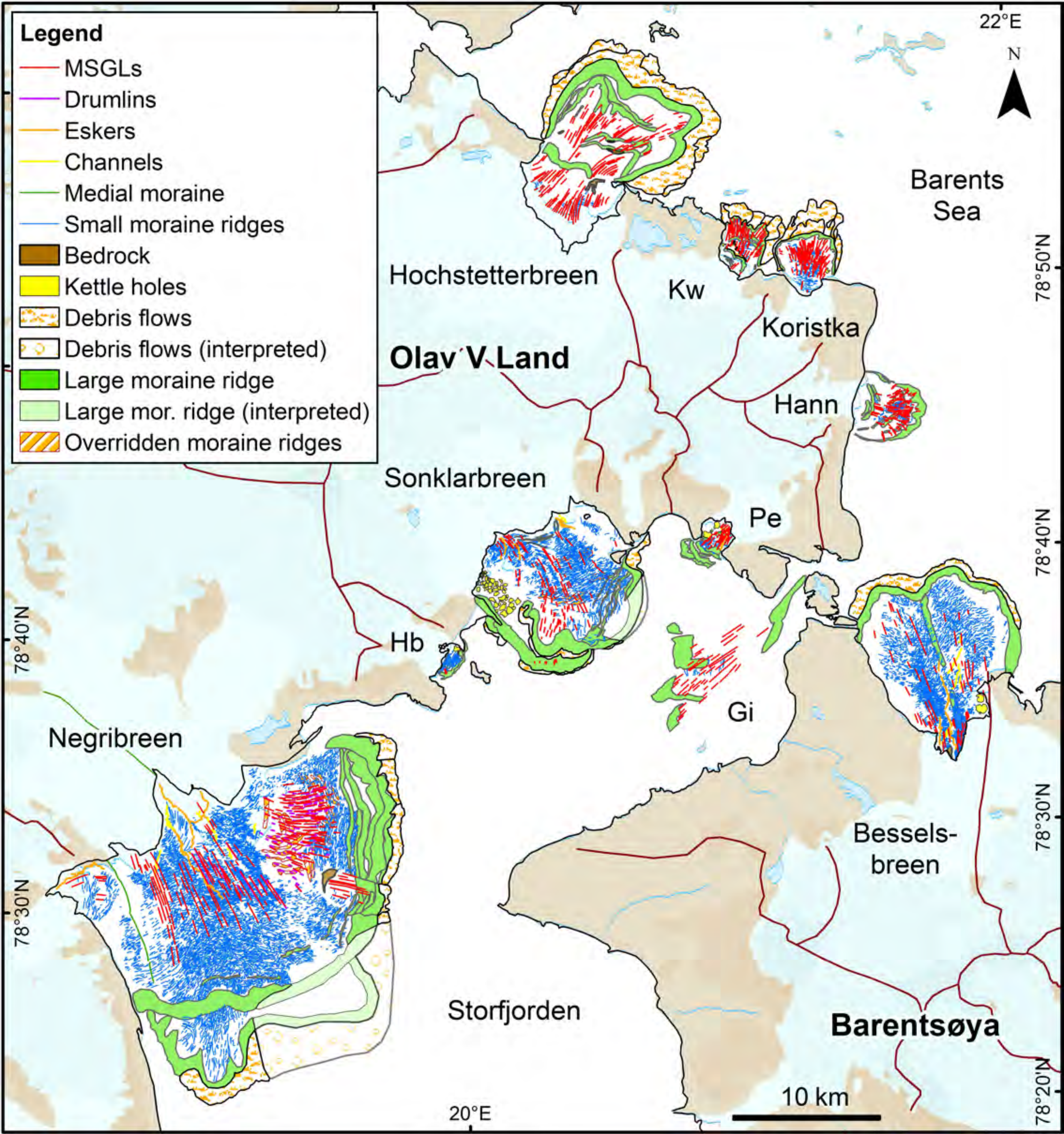

Legend
MSGLs
Drumlins
Eskers
Channels
Medial moraine
Small moraine ridges
Bedrock
Kettle holes
Debris flows
Debris flows (interpreted)
Large moraine ridge
Large mor. ridge (interpreted)
Overridden moraine ridges
22°E
N
Barents Sea
Hochstetterbreen
Kw
Koristka
Olav V Land
Hann
Sonklarbreen
Pe
Hb
Gi
Negribreen
Bessels-breen
Storfjorden
Barentsøya
10 km
20°E
78°50'N
78°40'N
78°30'N
78°20'N
78°40'N
78°30'N

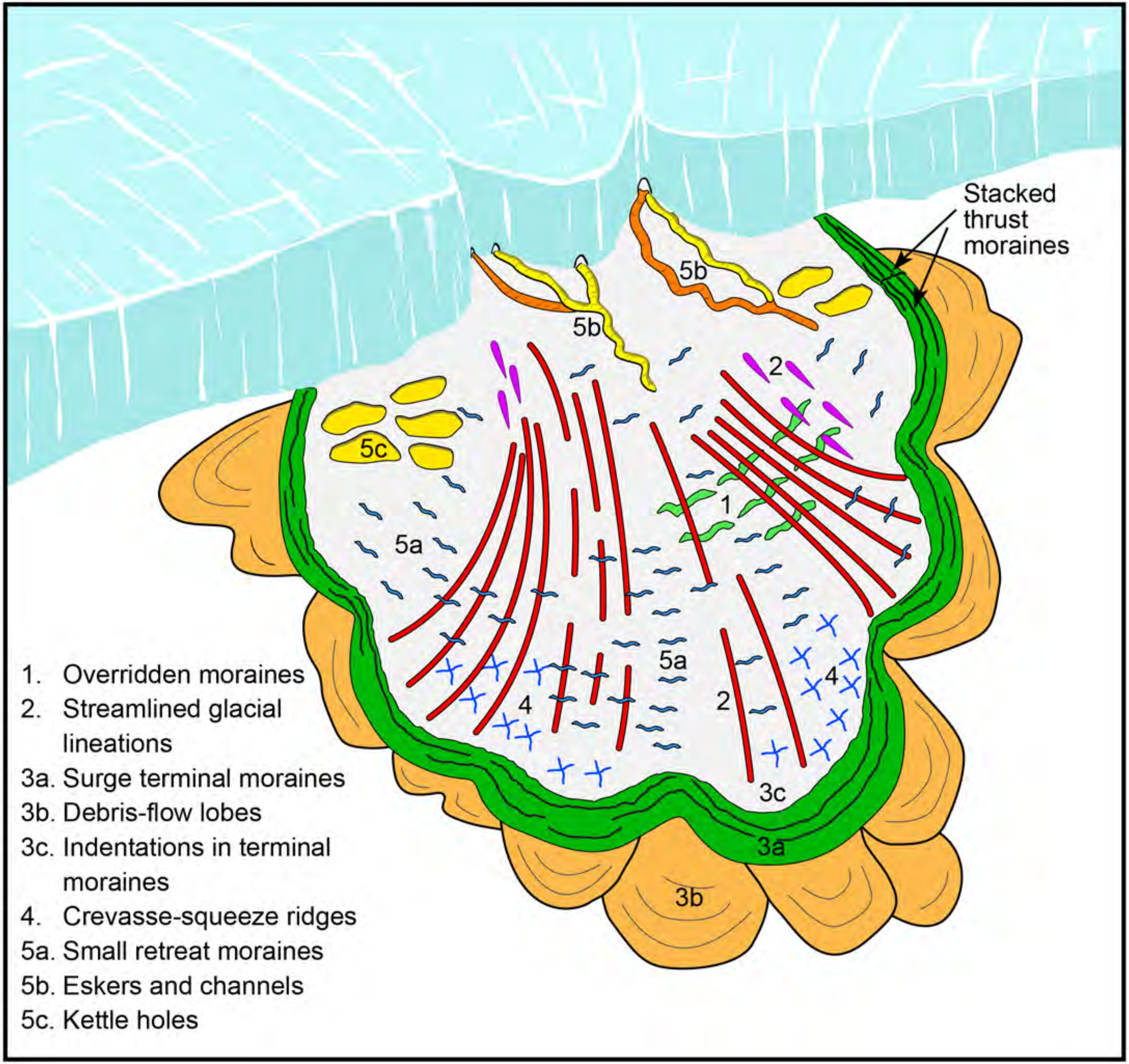

Stacked thrust moraines
5b
5b
2
5c
1
5a
5a
4
2
4
3c
3a
3b
1. Overridden moraines
2. Streamlined glacial lineations
3a. Surge terminal moraines
3b. Debris-flow lobes
3c. Indentations in terminal moraines
4. Crevasse-squeeze ridges
5a. Small retreat moraines
5b. Eskers and channels
5c. Kettle holes

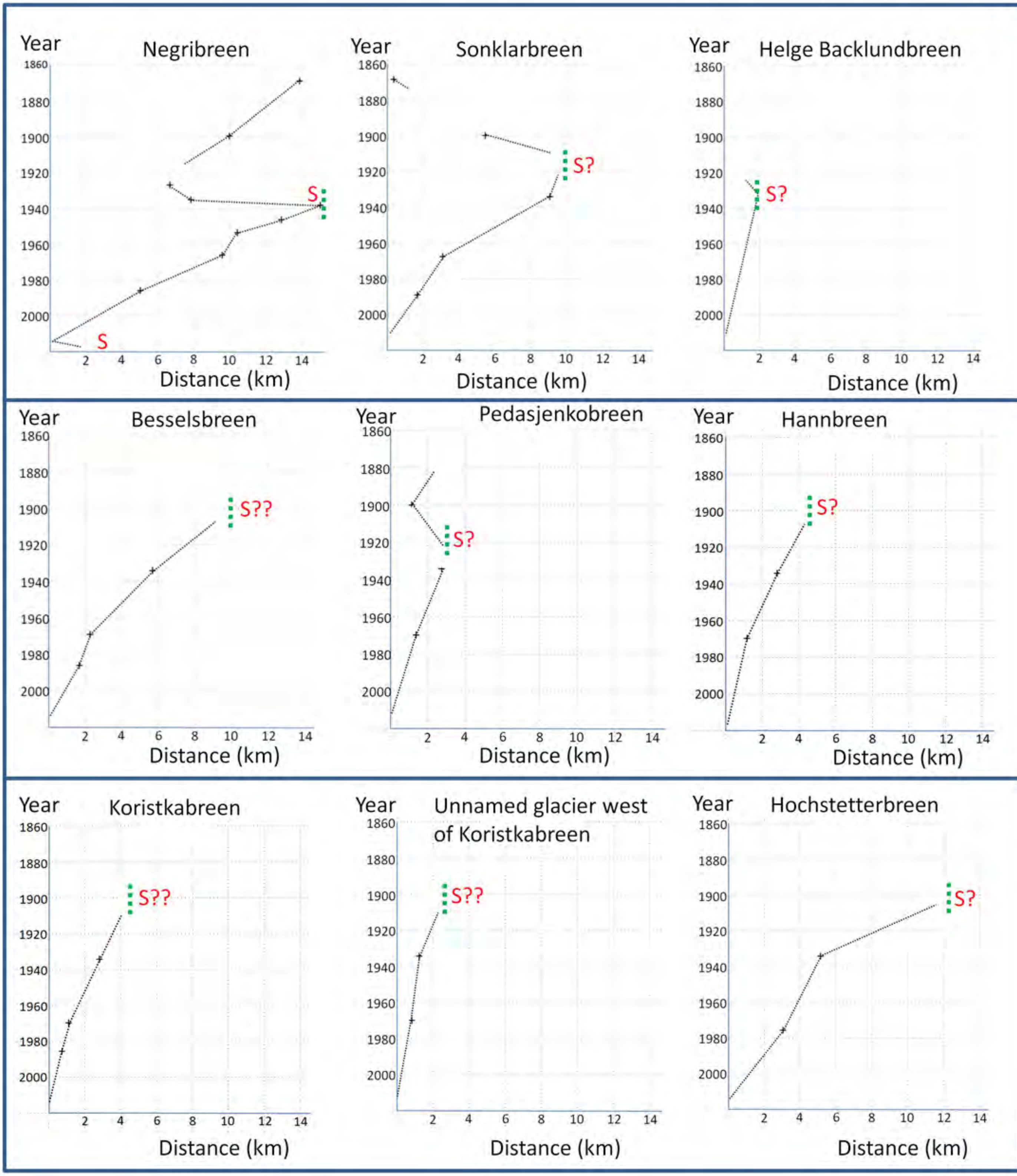
Year
Negribreen
S
S
Distance (km)
Year
Sonklarbreen
S?
Distance (km)
Year
Helge Backlundbreen
S?
Distance (km)
Year
Besselsbreen
S??
Distance (km)
Year
Pedasjenkobreen
S?
Distance (km)
Year
Hannbreen
S?
Distance (km)
Year
Koristkabreen
S??
Distance (km)
Year
Unnamed glacier west of Koristkabreen
S??
Distance (km)
Year
Hochstetterbreen
S?
Distance (km)
1860
1880
1900
1920
1940
1960
1980
2000
2
4
6
8
10
12
14

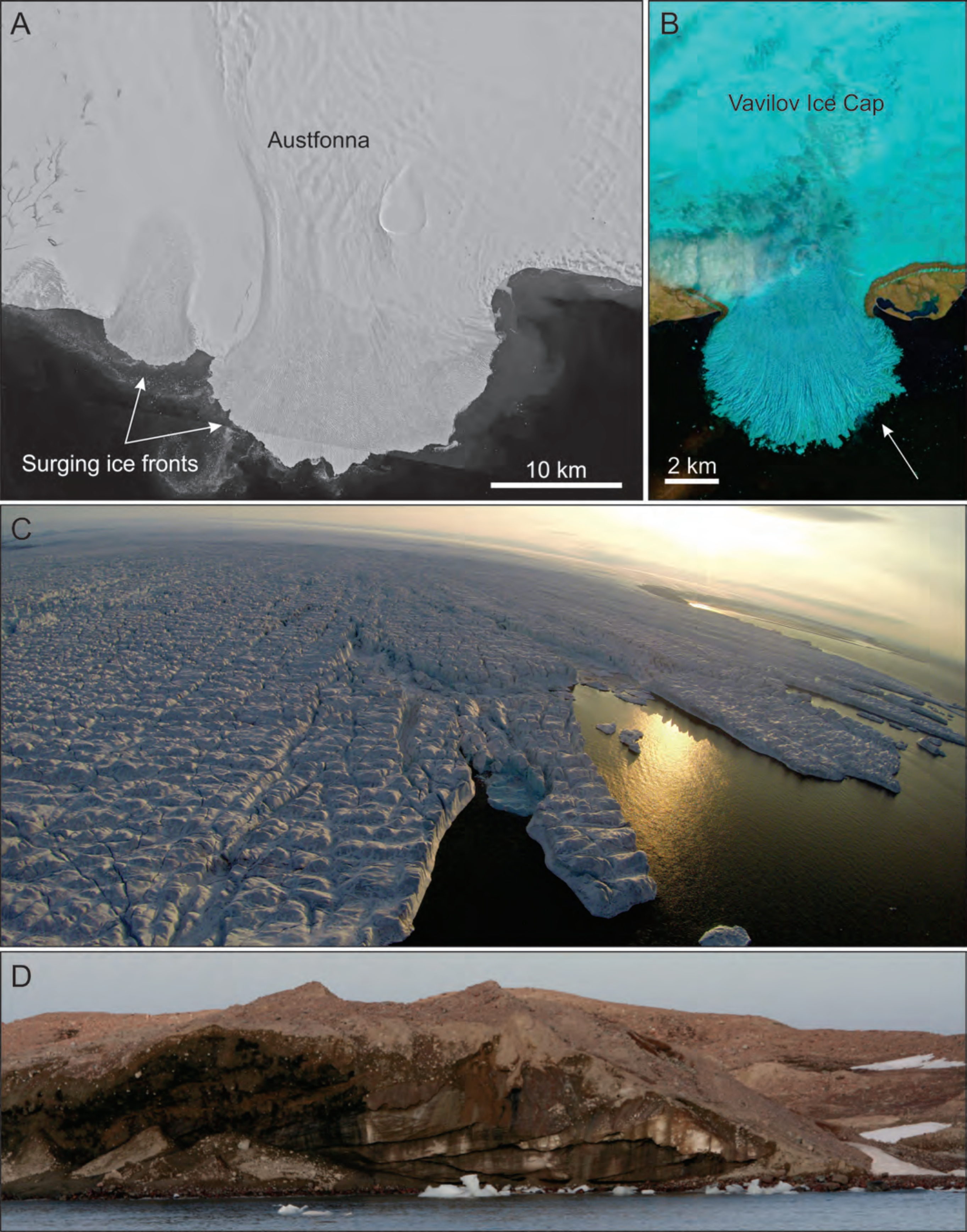
A
Austfonna
Surging ice fronts
10 km
B
Vavilov Ice Cap
2 km
C
D